https://doi.org/10.5194/egusphere-2026-2962
Preprint. Discussion started: 20 July 2026

High resolution rainfall estimation from Commercial Microwave Links in the city of Niamey in Niger

Modeste Kacou[1], Marielle Gosset[2], Iñigo Reizabal[2]

[1]Laboratoire des Sciences de la Matière, de l'Environnement et de l'énergie Solaire, Université Félix Houphouët-Boigny, Abidjan, 22 BP 582 Abidjan 22, Côte d'Ivoire

[2]Geoscience Environnement Toulouse (Université de Toulouse, IRD, CNRS, CNES), 31400, Toulouse

Correspondence to: Marielle Gosset (Marielle.gosset@ird.fr)

Summary < 500 characters

This paper illustrates that in regions that suffer from lack of meteorological information, the cellular phone network can provide rainfall measurement and mapping. This is illustrated in Niamey, the capital city of Niger using data provided by a telecom operator during 2017, a season marked by many intense rainfall. We analyse the microwave attenuation and transform it into rainfall maps, every 15 minutes, showing very high rainfall rates related to intense tropical convection.

Abstract. Commercial microwave links (CML) from cellular phone networks have become a source of opportunistic information on rainfall. In this study we use a dense network of 144 CMLs over the city of Niamey, in Niger, to estimate rainfall with a 15-minute resolution. The validation of these estimates with rain gauges shows that for links located within 2 km of a gauge the correlation of 15-minute time series is around 0.85, and the overall bias is low (0 to 10 % depending which link length and frequencies are considered). The CMLs are well suited to detect and quantify the intense rainfall rates associated with the mesoscale convective systems which bring most of the rain -and often floods- in the region. These good results are obtained with a simple and easily transferable processing chain. The study confirms the interest of CMLs in otherwise data scarce areas.

https://doi.org/10.5194/egusphere-2026-2962
Preprint. Discussion started: 20 July 2026

1. Introduction

Rainfall is one of the climate variables that impact most the environment and human activities. As the main entry to the continental hydrological cycle, rainfall variability over space and time controls water resources and hydrometeorological risks, floods or droughts. Accurate precipitation estimation is hence needed for research and applications, in meteorology, climate analysis, hydrology, agriculture. However, rainfall variability makes its measurement a challenge and in most of the earth surface the available observations are inadequate (Kidd et al., 2017). The most industrialized countries are equipped with dense networks of rain gauges and weather radars. Combining both sensors high resolution rain maps, with regular kilometric grids and infra-hourly time steps are routinely produced by weather services at country scale. Radar based data sets are useful for understanding the small spatial and temporal scales of extreme precipitation (Lengfeld et al., 2020). Unfortunately, radar networks are not available worldwide and the need for better rainfall estimation is acute in the tropics and singularly in sub-Saharan Africa. Sub-Saharan Africa is the continental surface with the overall scarcest rain gauge density (Kidd et al., 2017) and deficit of weather radar (Heistermann et al., 2013). This observational gap is all the more problematic that African countries are highly vulnerable to floods (Di Baldassarre et al. 2010, Tramblay et al. 2020, 2022) and population exposure is increasing (Belloni et al. 2021, Tellman et al. 2021) especially in urban areas. Flood risk is expected to grow further in the future years as the population density keeps on increasing while climate change causes rainfall intensification (Panthou et al., 2018 ; Taylor et al., 2017). One aggravating factor for urban floods in Africa is the convective nature of rainfall which produces intense and rapidly evolving rain fields (Roca and Fiolleau, 2020 ; Turko et al., 2021) leading to flash flooding.

In the last decades new measuring techniques based on opportunist sensors have emerged as a way to provide rainfall information complementing radars and gauges (Chwala et al., 2026). One of these opportunistic methods involves the use of commercial microwave links (CMLs) from mobile telecommunication networks. First introduced by Messer et al. (2006) and Leijnse et al. (2007), the technique makes use of the attenuating effect of rainfall on microwave propagation. This effect can be measured between the transmitting and receiving antennas of a cellular phone network liaison and then used for estimating rainfall. The technique was originally developed in Europe and Israel, where most of the algorithmic development to transform the raw signal into rainfall estimation and mapping originate (Chwala et al., 2026; Chwala and Kunstmann, 2019; Uijlenhoet et al., 2018). A few meteorological services in Europe, have been prototyping the integration of CML data into their operational rainfall products (Wenzel et al., 2023). In other regions CMLs use for rainfall is still more experimental but the number of related studies is increasing, with recent experiments in China (Pu and Liu, 2024; Song et al., 2021) and under tropical climate in Sri Lanka (Overeem et al. 2021; Walraven et al. ,2024).

In Africa, few experiments with limited data sets were also reported. Doumounia et al., (2014) obtained interesting results in Burkina Faso, based on a single link of 7 GHz and around 30 km, which lead to organizing the first conference on CML in Africa (Gosset et al., 2016). Djibo et al. (2023) exploited 259 links (10 to 13 GHz and 0.2 to 7.6 km) over the capital of Burkina Faso Ouagadougou to assess CML based 5-minutes rainfall maps, but with only a single rain gauge with daily rain measurement for validation. Over Kenya, David et al. (2021) discussed potential applications of CML for agriculture based on

https://doi.org/10.5194/egusphere-2026-2962
Preprint. Discussion started: 20 July 2026

4 links. So far, the validation of the CML technique under tropical climate has been limited by the lack of access to high resolution rain gauges needed for the analysis of the performance at sub-daily time scales and for assessing the ability of CMLs to accurately estimate intense convective rainfalls.

This study presents results obtained with a dense network of 144 microwave links over the city of Niamey in Niger. The CML data is provided at 15 minute step using the operator's own network monitoring system (NMS) and unlike other studies in Africa, we had access to quality controlled reference rain gauge data with 5 minute time steps, allowing the evaluation of the CMLs at a high time resolution The study is carry out for the rainy season 2017 when many intense rainfall events and flooding occurred in Niamey. Rainfall estimation from the microwave links is produced for all the major rainy events of the season, representing a total of 55 hours of rainfall. This is one of the first quantitative evaluation of the CML technique in Africa at short time step with such a large data set.

Section 2 presents the study region, the CMLs network and validation data, section 3 introduces the method used to transform the signal levels provided by the operator into rainfall rates, section 4 presents the quantitative results, section 5 the conclusion and perspectives.

2. Study area and Data

The study area is Niamey, the capital of Niger. Niamey lies into the Sahelian, semi-arid eco-climatic zone. The region is known for its intense climate variability and the long-lasting drought of the 1970–2000 period. In recent years the area has been subjected to intense rainfall and flooding (Casse et al., 2016; Panthou et al., 2018) and studies suggest an intensification of the rainfall regime (Mahamadou et al., 2026).

The rainy season is relatively short, 4 months on average from mid-June to mid-October in relation with the position of the Inter Tropical Convergence Zone (ITCZ). During the West African Monsoon season, most of the rain is brought by organized Mesoscale Convective Systems (MCSs) (Mathon et al., 2002; Roca and Fiolleau, 2020, Guehi et al., 2026). MCSs are characterized by a front of convective cells followed by a more spread stratiform part (Alcoba et al., 2016; Cazenave et al., 2016; Houze, 1988; Vischel et al., 2011). Typically, at a given point, the convective rain lasts about an hour, with peak rain rates reaching 100 to 150 mm/h, the stratiform rain that follows is usually below 5-10 mm/h, and lasts for several hours (Moumouni et al., 2008; Müller et al., 2018). The convective rain accounts for 75-80% of the total rainfall. These intense rain rates are responsible for pluvial floods and need to be monitored, however their high spatial variability is a challenge for observation (Turko et al., 2021; Vischel et al., 2011).

https://doi.org/10.5194/egusphere-2026-2962
Preprint. Discussion started: 20 July 2026

2.1. Commercial microwave links

The commercial microwave link data was originally obtained through a collaboration with the mobile telecommunication operator Orange (the network has now been bought by Zamani Com). The data was obtained in the framework of the project ‘Rain Cell Africa - Niger’ financed by the World Bank Global Facility for Disaster Reduction and Recovery (WB-GFDRR) in order to test the potential of the CML based rainfall technique for urban hydrology in Africa, following the promising results of Doumounia et al. (2014) using a single link in Ouagadougou.

The meta-data provided by the operator contains the information necessary to locate the antennas’ positions and process the raw data and derive rainfall rates. The main information is the position of the transmitting and receiving antennas, and the frequency of operation. Additional information may help in the interpretation of the results (type of equipment and radome ; polarization ; antennas height, angle and model).

The geographical layout of the available network is superimposed on the map of Niamey in Figure 1a, together with the position of the rain gauges. We can observe a homogeneous spatial distribution of links with the urbanized part of the city of Niamey. For some CMLs (not shown in Figure 1) the Meta-Data was incomplete, hence they could not be included in the study.

https://doi.org/10.5194/egusphere-2026-2962
Preprint. Discussion started: 20 July 2026

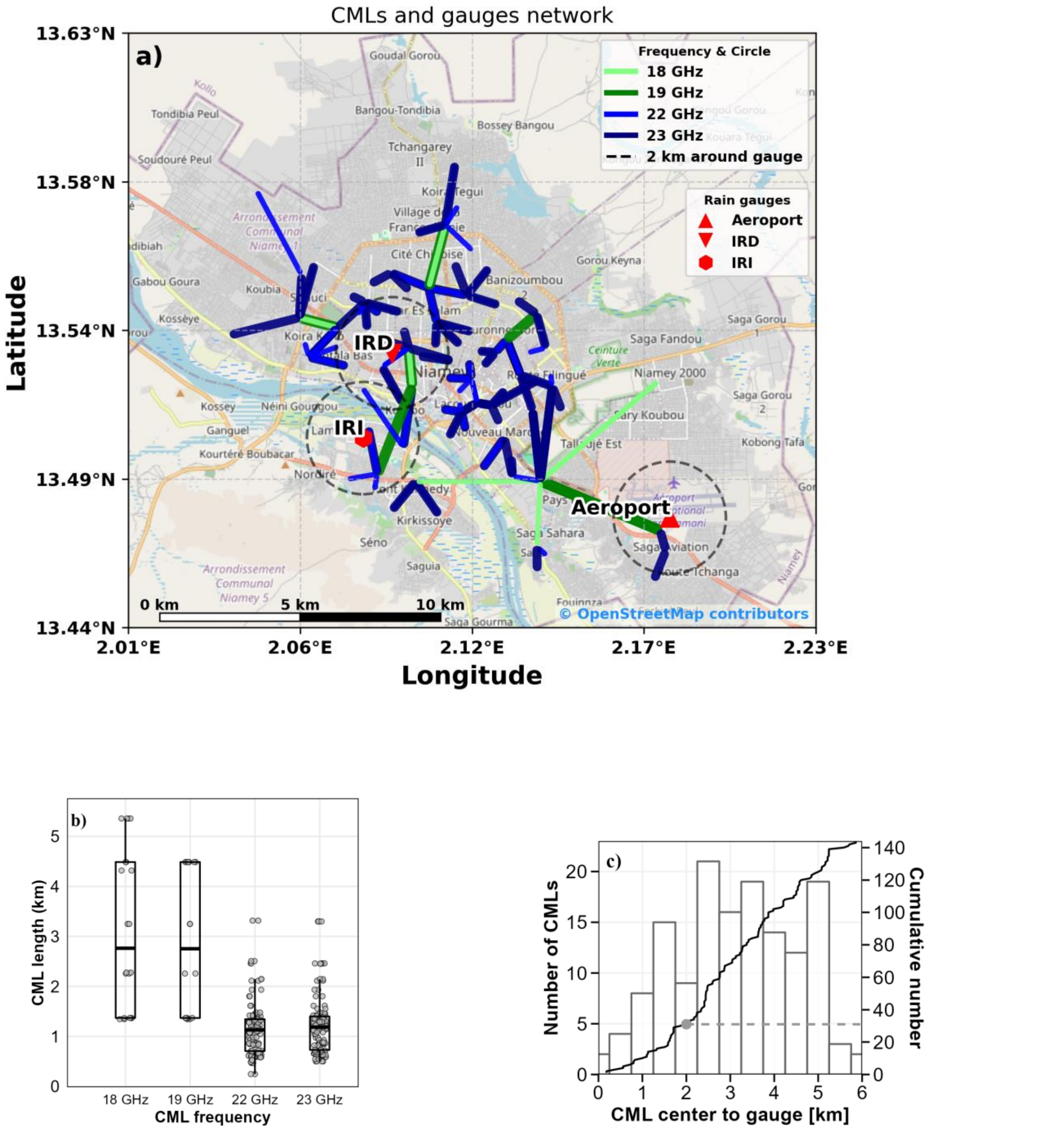

https://doi.org/10.5194/egusphere-2026-2962
Preprint. Discussion started: 20 July 2026

Figure 1: a) Positions of the CMLs (blue et green lines depending on frequency, as indicated) and gauges (red). b) Distribution of the link lengths (Y axis) as a function of their frequency (X axis).
c) Distribution of the distances between the links (center) and their closest gauge.

As displayed in Figure 1, the link lengths range from 0.245 to 5.36 km, with most links in the range 0.5-2 km (Figure 1b). Most links (126) operate at 22 or 23 GHz, and only 18 links at 18 or 19 Ghz. For some of the pairs of antennas or link lines represented in Figure 1, two sub links are available, in the two opposite directions (as each pylon hosts both transmitters and receivers) and they may operate at slightly different frequencies (or in different polarizations, but this information was not available). Altogether 144 CMLs corresponding to 86 antenna pairs positions could be exploited.

The distance of the links compared to the nearest rain gauge are shown in Figure 1c. Here the considered distance is to the center of the link (other measures like the distance to the closest antenna, or the perpendicular distance to the link path, could be considered). With this measure, 31 links are less than 2 km away from their closest gauge. The data provided by the operator for all links are the received signal levels (RSL) every 15 minutes. For some links, the transmitted signal levels were also provided. The inspection showed that the TSL are constant, very stable and consequently only the RSL are used -as in most studies (Chwala et al., 2012; Imhoff et al., 2020; Ostrometzky and Messer, 2018; Overeem et al., 2011a; Pu and Liu, 2024)- in order to process all links with a similar processing. The data is provided at the end of each time step and contains the mean, minimum and maximum value of RSL recorded in the last 15 minutes. For the present work we used only the mean RSL information. The data was provided with a 1 dBm precision.

Among the recorded data, 2017 is the year with the most complete record (data for all CMLs being transmitted every 15 minutes). The data has been analysed during the rainy season, from May to August, when rain gauge data was available.

2.2. Rain gauges and rainfall events

Two rain gauges from the the African Monsoon Multidisciplinary Analysis (AMMA)–Couplage de l'Atmosphère Tropicale et du Cycle eco-Hydrologique (CATCH) observatory (AMMA-CATCH, 1990; Galle et al., 2018) are situated within Niamey's agglomeration, and close to several links, a third gauge is located at the airport, more east, as shown in Figure 1. The two central gauges (IRI and IRD) are 3 km apart, the Airport gauge is 11 km from IRD. The rain gauges are tipping bucket (0.5 mm resolution) and the rain rates have been recorded with a 5 minute time step. For the comparisons with the CMLs time series, the rain rate is averaged over 15 minutes.

2017 was a difficult year regarding the security conditions and the data collection and network maintenance was not as frequent as usual. The record is therefore incomplete (some days missing; station stopped). However, the 10 major rainfall events (representing 75% of the total rainfall that year) that occurred in 2017 were recorded by the two central gauges. One of the events was also recorded by the airport gauge.

https://doi.org/10.5194/egusphere-2026-2962
Preprint. Discussion started: 20 July 2026

The date, length and rainfall characteristics of the 10 major events recorded by the gauges in Niamey from May to August 2017 are listed in Table 1. The events vary in length (from 45 minutes to 11 hours), rainfall accumulation and intensity. Despite their proximity the gauges have recorded very different accumulations or maximum intensity for some events (highlighted in Table1). This is consistent with the rapid spatial decorrelation of the rainfall structure which has been reported before for African convective systems (Guilloteau, 2016; Israelsson et al., 2020) and has to be kept in mind when the rain gauge are compared with the CML estimation.

Rainfall events	Start (UTC)	Duration(in hours:minute)	Gauge name	Total Rainfall Amount (mm)	Maximum rain rate (mm/h)
event_1	11/05/2017 02:45	05:30:00	IRD	51.44	**57.8**
	11/05/2017 03:00	04:30:00	IRI	51.93	**32.76**
event_2	13/06/2017 18:45	10:15:00	IRD	113.5	**80.44**
	13/06/2017 18:45	11:30:00	IRI	94.89	**98.72**
event_3	19/06/2017 17:15	00:45:00	IRD	42.67	**88.28**
	19/06/2017 17:30	00:45:00	IRI	42.01	**110.2**
event_4	04/07/2017 00:00	04:45:00	IRD	**54.36**	**63.52**
	04/07/2017 00:00	05:00:00	IRI	**86.8**	**112.16**
event_5	06/07/2017 02:00	07:45:00	IRD	**28.4**	58.52
	06/07/2017 02:00	07:45:00	IRI	**35.53**	60.4
event_6	22/07/2017 03:45	04:15:00	IRD	**42.46**	**57.72**
	22/07/2017 03:30	04:45:00	IRI	**65.48**	**91.32**
event_7	07/08/2017 19:00	03:00:00	IRD	21.99	**37.72**
	07/08/2017 19:00	03:15:00	IRI	19.43	**29.72**
event_8	23/08/2017 02:45	**11:15:00**	IRD	**48.91**	78.88
	23/08/2017 06:30	07:30:00	IRI	**76.04**	90.28
event_9	26/08/2017 04:30	04:00:00	IRD	56.49	90.88
	26/08/2017 04:30	04:00:00	IRI	58.71	82.28
event_10	30/08/2017 17:45	00:45:00	Aéroport	**18.23**	**36.88**
	30/08/2017 17:30	01:15:00	IRD	**19.25**	**28.52**
	30/08/2017 17:45	01:00:00	IRI	**11.01**	**15.56**

Table 1 : characteristics of the 10 major rainfall events recorded in 2017 by the rain gauges. When the total amount or maximum rain rates differ by more than 20 % among the gauges, they are highlighted in bold.

https://doi.org/10.5194/egusphere-2026-2962
Preprint. Discussion started: 20 July 2026

Note that Rain Gauge at the airport (Aéroport) was operationnal only on the last event.

3. Rainfall estimation from the commercial microwave links

This section provides the details of the processing chain to convert the raw data provided by the operators into rain rates.

3.1. Basic principles – k-R relationship and path integrated attenuation

The principle of rainfall measurement from the path integrated attenuation measured between the two ends of a microwave link has been explained by several authors (Yapi et al., 2023; Zhang et al., 2023).

The basis, is the existence of a simple analytical relationship between the specific attenuation *k* [dB/km] along a rainy path and the rain rate *R* [mm/h] :

$$k=a\,R^{b} \tag{1}$$

The attenuation of electromagnetic waves as they propagate through a rainy path, is due to effect of all the individual drops which absorb and scatter in all directions, the electromagnetic waves. This is why, the amount of attenuation along the path is closely related to rain rate. The fact that Eq. 1 takes the form of a power law is related to the rain drop size distributions, and their evolution through microphysical processes (Atlas and Ulbrich, 1977; Esmaeil Nia and Shokri, 2025; Olsen et al., 1978; Upton et al., 2005). Both the telecommunication and meteorological communities (in particular weather radar specialists) have analysed, modelled or fitted empirically, k-R relationships (Berne and Uijlenhoet, 2007; ITU-R, 2005) for different frequencies and/or climate regions. They have shown that in the frequency range 15-30 Ghz *b* is close to 1, making the k-R relationship quasi-linear.

Here the k-R relationships for the frequencies of the provided CMLs, 18-19-22-23 GHz were calculated on the basis of the Mie theory for electromagnetic scattering by spherical particles (Mie, 1908) and using rain drop size distributions (DSDs) recorded in African MCSs (Moumouni et al., 2008). The derived coefficients *a* and *b* are listed in Table 2. As expected, *b* is very close to 1; the values of *a* are also very closed to those proposed in the literature (Berne and Uijlenhoet, 2007; ITU-R, 2005).

Frequency (GHz)	a	b
18	0.0781	1.0654
19	0.0873	1.0600
22	0.1171	1.0471
23	0.1281	1.0428

Table 2 : Coefficients *a* and *b* of the k-R relationship used in this study, based on the Mie theory and drop size distributions from Moumouni et al. (2008); see text.

https://doi.org/10.5194/egusphere-2026-2962
Preprint. Discussion started: 20 July 2026

A microwave link of length L [km] measures the path integrated attenuation (PIA) due to rain between its two ends, which according to Eq. 1 is :

$$A_{rain} = PIA = \int_0^L k(s)ds \approx a\overline{R}^b L \quad (2)$$

With k(s) the specific attenuation at range s, $\overline{R}$ the path averaged rain rate. The approximation in the last member of Equation 2 is only valid if the exponent b equals 1 or if the rain rate is constant along the path ($R = \overline{R}$).

3.2. **Raw attenuation and baseline**

The raw attenuation between the transmitting and receiving ends of a link is measured as the difference between the transmitted (TSL) and received (RSL) signal levels provided by the operator.

$$A_{raw} = TSL - RSL \quad (3)$$

When the information on TSL is not available or when it is constant, the monitored raw attenuation -as used for the present work- is :

$$A_{raw} = -RSL \quad (4)$$

In the absence of rain, A_{raw} is relatively stable. However, even in non rainy conditions, A_{raw} varies for different reasons like dew on the antennas or variation in the refractive index of the air or attenuation by atmospherics gazes; changes in the transmitted power levels or more generally noise in the electronics or the signal (quantization) (Chwala and Kunstmann, 2019; Harel et al., 2015; Henning and Stanton, 1996; Leijnse et al., 2007; van Leth et al., 2018; Ostrometzky and Messer, 2018; Overeem et al., 2011a; Pu and Liu, 2024). What is important for rainfall estimation is not the absolute value of A_{raw} but its variations in presence of rain.

In order to quantify the amount of attenuation due to rain, the reference level or baseline A_{base} representative of dry conditions must be estimated, and A_{rain} estimated as:

$$A_{rain} = A_{raw} - A_{base} \quad (5)$$

Errors in defining the baseline level are a major source of uncertainty in rainfall estimation from microwave links (Schleiss and Berne, 2010a; Zinevich et al., 2010) and can lead to serious biases when the baseline is systematically under- or overestimated.

Baseline estimation has been the subject of many articles (Fenicia et al., 2012; Ostrometzky and Messer, 2018; Overeem et al., 2011a; Rahimi et al., 2003; Upton et al., 2005; Zinevich et al., 2010) and a variety of methods have been proposed. The complexity of the problem depends on many factors like the atmospheric conditions which can lead to dew deposit on the

https://doi.org/10.5194/egusphere-2026-2962
Preprint. Discussion started: 20 July 2026

antennas and strong diurnal cycle (Kumah et al., 2021; Schleiss and Berne, 2010a). The complexity of the processing method which should and can be used to determine the baseline depends also on the type of data available, its precision and sampling. For instance, spectral methods (Chwala et al., 2012) are powerful to distinguish the dry and wet period on very high-resolution time series (12 sec apart) while simpler methods based on variance analysis (Doumounia et al., 2014; Schleiss and Berne, 2010b) seems sufficient on data with larger time steps (15 min).

The atmospheric conditions in Sahel and the characteristics of the data, lead us to implement a relatively simple method for baseline determination, as illustrated in Figure 2. As discussed in section 2, the region is in semi-arid conditions, rainfall is due to a small number of relatively short (a few hours) and intense systems. Most of the time, even during the rainy season, the conditions are dry. The initial analysis of the raw time series during the wet and dry periods (defined by the closest rain gauge) show that the signal is very stable outside rain – or at least the fluctuations are smaller than the 1dBm signal resolution which is provided. Testing different methods (wet/dry classification based on variance) and parameters (threshold ; length of processing time window), lead us to use the mode of the A_{raw} distribution within a 24 hours window preceding the current time step, as definition of the baseline. This method was chosen for its skill and its simplicity of implementation (with operational transfer in mind).

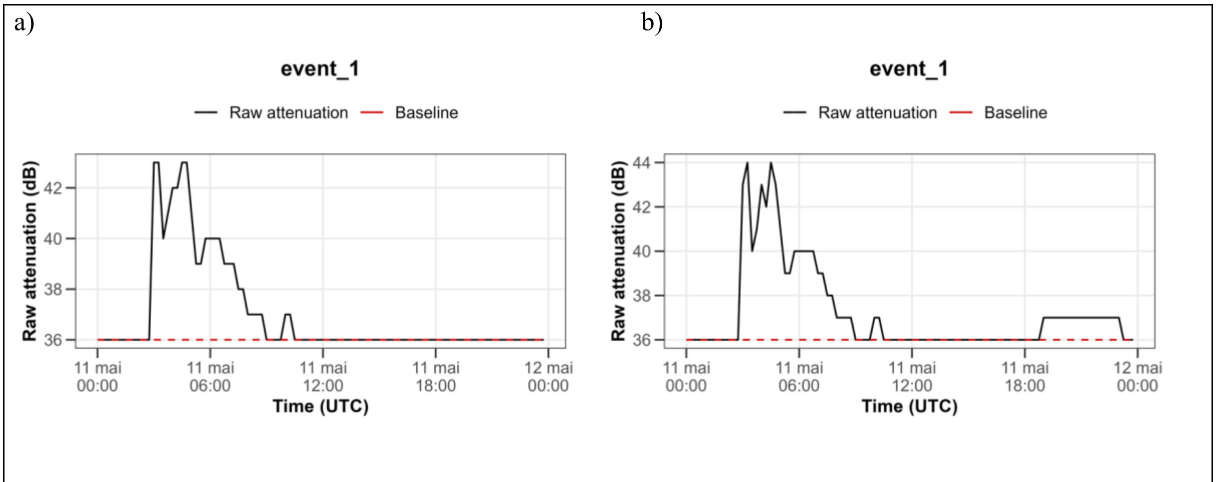

Figure 2 : illustration of the baseline (red) estimated as the mode of the raw attenuation (black) over a 24 h period. The example is for two different links during the first event.

Once the baseline is determined with the mode method, A_{rain} is calculated (Eq. 5) and a first basic estimation of the rain rate is done for each link by inverting Equation 2:

https://doi.org/10.5194/egusphere-2026-2962
Preprint. Discussion started: 20 July 2026

$$R_{CML} = (A_{rain}/aL)^{(1/b)} \quad (6)$$

The figures 3 and 4 display heat maps illustrating the time evolution of the rain occurrence (Fig. 3) and the rain rate (Fig. 4) measured by the links and the gauges as a MCS was passing over Niamey. The example is for the first major rain event that occurred on May 11th 2027, started just before 3 am and lasted about 5 hours (Table 1). Each horizontal row is associated with one sensor, with the 144 CMLs in the top plots (*a, b*) and the 2 functioning rain gauges below (*c, d*). The links are sorted by decreasing length along the Y axis – with the longest link at the bottom.

The left plots (*a, c*) show the time evolution of the rainfall estimated by all sensors while the right plots (*b, d*) show the average value per event, with the number of rainy time steps (above 0.1 mm/h) in Fig. 3 *b* and *d*, and the mean rain rate in Fig 4 *b* and *d.*

Figures 3 and 4 provide a visual overview of the overall agreement between the links and the gauges in terms of capturing the dynamics of the rainfall event over Niamey. A majority of links are in good agreement with the gauges for the amount of rainy steps (Fig 3*b, d*) and the timing of the event (Fig 3*a, c*). Figure 4 shows however that this initial rainfall estimation tends to overestimate the rain rates, even if the typical structure of the MCS with heavy convective rain rates (dark blue) followed by lower stratiform rain (lighter blue) is reproduced. The overestimation is much more marked for the shortest links (top of Fig. 4a and b) than for the longest. Another feature in Figures 3 and 4 is the false detection of rain after the event, up to a few hours for some of the links. There are also links behaving as outliers with unrealistic high rain rates (above 200 mm/h, red pixels) and links which didn’t detect any rain.

The next two sections explain how the next steps in the processing, outliers elimination and wet antenna correction improve CML estimation.

https://doi.org/10.5194/egusphere-2026-2962
Preprint. Discussion started: 20 July 2026

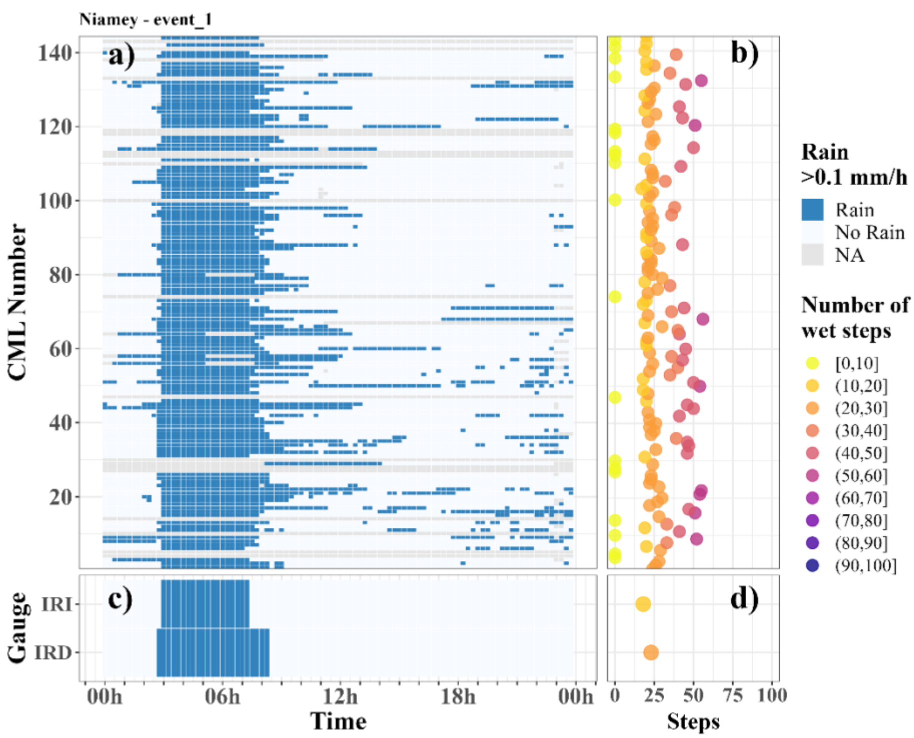

Figure 3 : a) Illustration of the time evolution of the rain detected by the network of links and gauges for the May 11th event. On the left plots, blue pixels indicate that rain rate above 0.1 mm/h was measured for the correspond 15 minute time steps, by one of the 144 CMLs (*a*) or the 2 gauges (*b*). The links are sorted by decreasing length along the Y axis – with the longest link at the bottom. The dots (color and position) on the right plots show the number of rainy time steps (above 0.1 mm/h) recorded during the event by each link (*b*) and gauge (*d*).

https://doi.org/10.5194/egusphere-2026-2962
Preprint. Discussion started: 20 July 2026

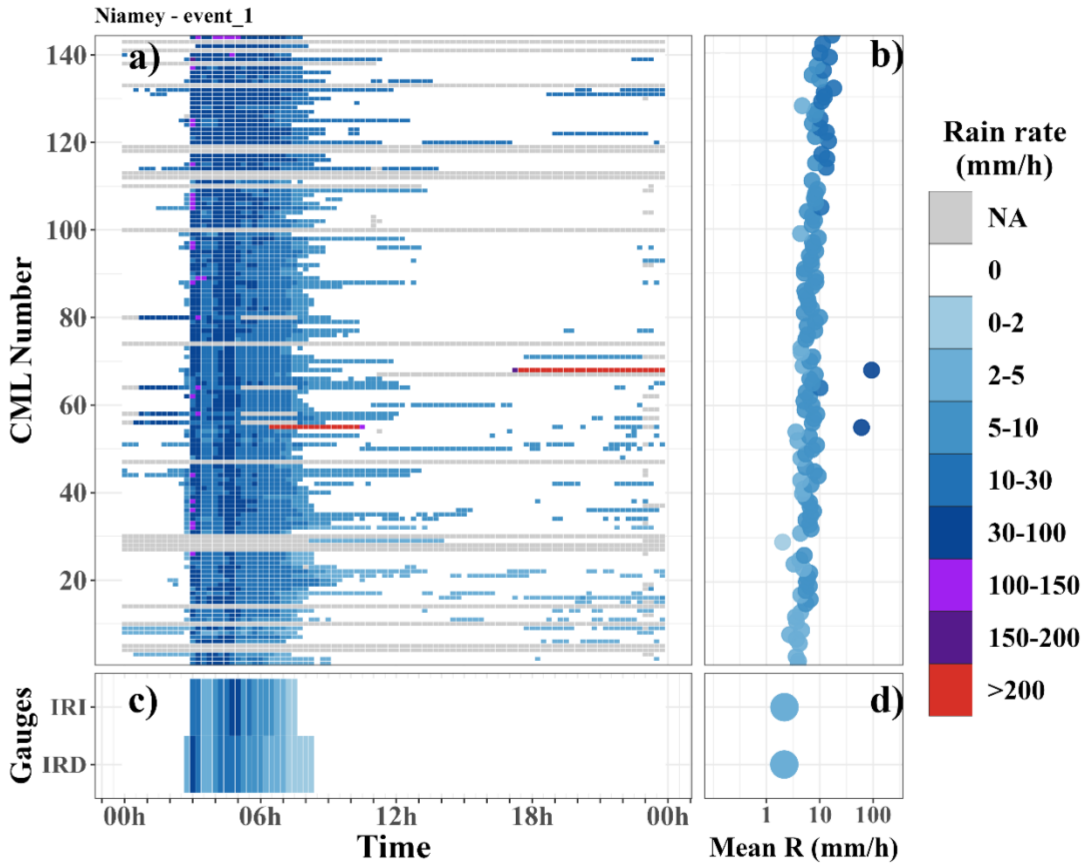

Figure 4 : a) Illustration of the time evolution of the rain rates over the network of links and gauges for the May 11th event. The pixel colour indicates the rain rate recorded by the 144 CMLs (*a*) or the 2 gauges (*b*). The links are sorted by decreasing length along the Y axis – with the longest link at the bottom. The right plots show the mean rain rate recorded for the event by each link (*b*) and gauge (*d*).

3.3 Outlier links filtering

Given the spatiotemporal structure of rainfall, and the proximity of the links (Fig 1a) some consistency is expected among neighbouring links. Some authors use this consistency to determine the rainy/dry periods (Overeem et al., 2016; Roversi et al., 2020).

Despite the overall synchronicity of the links and gauges, horizontal grey and red lines, standing out from the background pattern, are visible in Figure 4. They show a few links behaving as outliers, either because they stopped working or because

https://doi.org/10.5194/egusphere-2026-2962
Preprint. Discussion started: 20 July 2026

the attenuation values are very high, leading to unrealistic rain rates, above 200 mm/h. The values are too high to be attributed to antenna wetting, and the operator engineers suggest a problem with the sealing of the antenna radome, which can fill up with water inside, in case of very heavy rain and strong winds.

Based on the analysis of whole the data set, it was determined that the main type of problem is sudden overestimation and extreme values. For the current study, a simple filter based on a maximum acceptable rain rate was implemented. Based on the distribution of rain rates observed over 30 years by the gauges, a conservative maximum acceptable value of 250 mm/h was set. Links which show a correlation of less than 0.5 compared to the median of all other links within 5 km are also disregarded.

3.4 Wet antenna attenuation analysis

Figure 4 shows that rainfall following the initial convective rainfall is overestimated by the links, and from visual analysis it appears that the overestimation is stronger for the shorter links (upper part of the heat maps). Wet antenna attenuation is a possible candidate to explain this feature.

Many experiments with commercial or dedicated microwave links have shown evidence of attenuation of the microwave signal by the membrane that protects the antennas, as observed also with the radomes of weather radars. This wet antenna attenuation (WAA), introduces a positive bias in the estimation of rainfall from Eq. 2 which should be rewritten,

$$A_{rain} = A_{WA} + PIA = A_{WA} + aR^{b}L \qquad (7)$$

With A_{WA} the attenuation due to the wet antennas.

Several models have been proposed for the WAA, some studies consider a fixed value, others a dependency on frequency (WAA increases with frequency), or on rain rate, or both. The WAA also depends on the type of equipment used by operators and no universal model could be proposed so far. In practice, most retrieval algorithms introduce a parametric formula for a fixed or variable WAA and calibrate the parameter(s) empirically (Fencl et al., 2019; Leijnse et al., 2008; Ostrometzky et al., 2018; Schleiss et al., 2013)

In order to investigate WAA we analyse, for each link situated within 2 km of a gauge, the difference between the attenuation by rain estimated with the link A_{rain} (Eq. 5, 6) and the PIA which is expected given the rain rate measured by the gauge, PIA_{Gauge}:

$$PIA_{Gauge} = a\, R_{Gauge}^{\;b}\, L_{CML} \qquad (8)$$

with R_{Gauge} the rain rate measured by the rain gauge, *a* and *b*, from Table 2 for the frequency of the considered link and L_{CML}, its length.

Based on Equation 7, the difference between A_{rain} and the PIA can be attributed to WAA, on the assumption that i) R_{Gauge} is a good proxy for the average rainfall along the link path and ii) the parameters *a* and *b* are correct.

The scatter plots in Figures 5a and 5b display A_{rain} versus PIA_{Gauge} for all the available time steps of all links situated within 2 km of their closest gauge, for the two ranges of frequencies, 18-19 GHz and 22-23 Ghz. Altogether 29 CML-gauge pairs are considered with a minimum of 40 time steps each. The plot shows an overestimation of the attenuation by the CML and

https://doi.org/10.5194/egusphere-2026-2962
Preprint. Discussion started: 20 July 2026

suggests the existence of an additive component to the overall bias, which is expected from a WAA component (and not so much from unsuitable values of the *k-R* coefficients *[a, b]*). The intersect parameter of the fitting line is about 2.5 dB for the 18-19 GHz and slightly higher for 22-23 Ghz. An underestimation of the baseline would also create an addition bias, however the statistics on rain/no rain detection, discussed in section 4, show a low false alarm rate suggesting that the bias in Fig. 5 is induced by WAA rather than baseline underestimation. This is further highlighted in Fig. 5c which analyses the relative difference, (A_{rain}- PIA_{Gauge})/PIA_{Gauge} per classes of link length, exhibiting larger relative errors for the shortest links as expected from WAA.

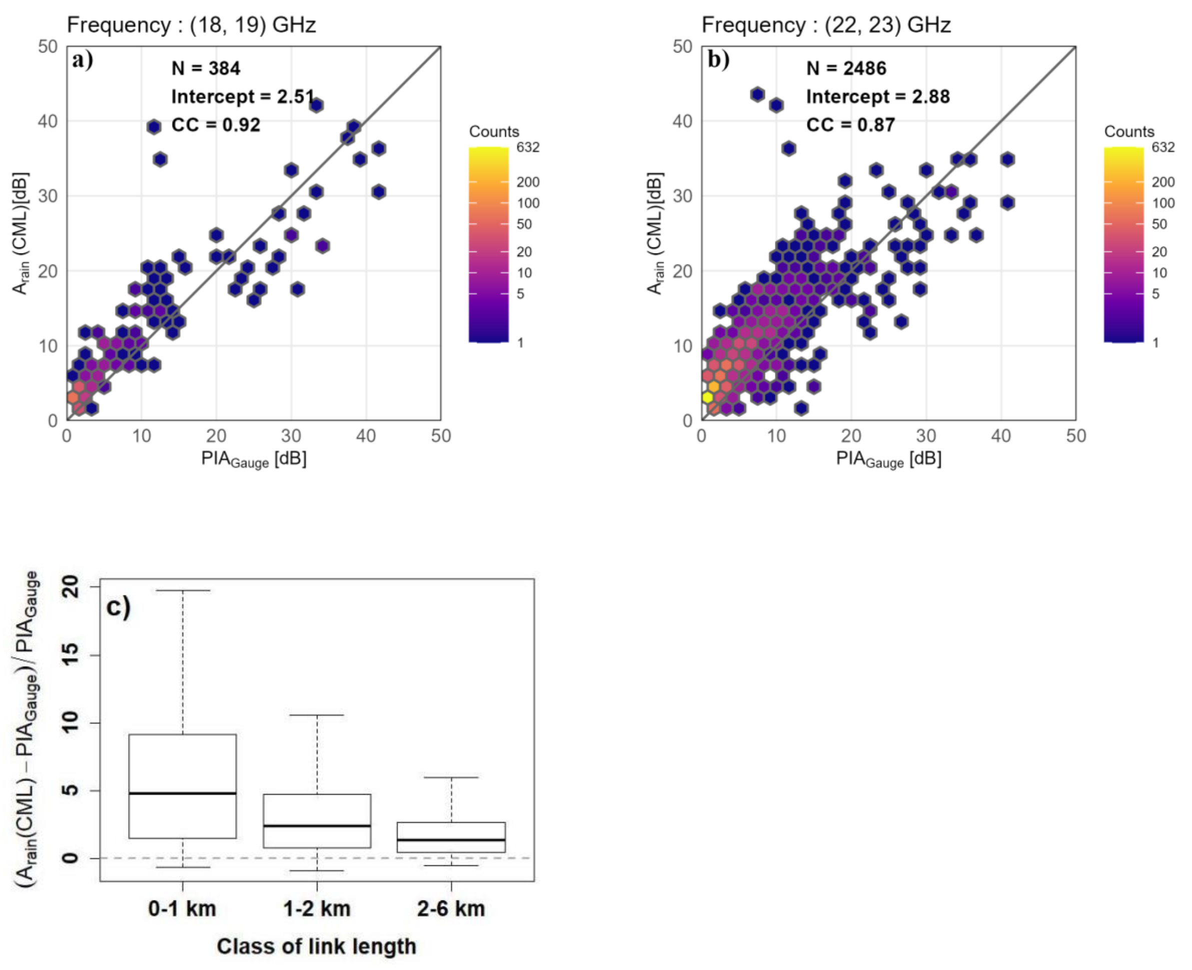

Figure 5 : Analysis of the difference between the attenuation by rain (A_{rain}) estimated with the CMLs and the PIA expected given the observed rain rate (PIA_{Gauge})-see text.

https://doi.org/10.5194/egusphere-2026-2962
Preprint. Discussion started: 20 July 2026

a) and b) scatter plot of A_{rain} versus PIA_{Gauge} for the frequency ranges, 18-19GHz (a) and 22-23 GHz (b). c) percentage of residual attenuation, $(A_{rain}$- $PIA_{Gauge})/PIA_{Gauge}$, for the indicated classes of CML length.

To further investigate which analytical form can be used to model the WAA we analyse the residuals, A_{rain}- PIA_{Gauge} as a function of the rain rate measured by the gauge. For this analysis we gathered the links from both frequency range, given that there are too few 18-19 Ghz links to have a robust model and the scatter plots of Figures 5a and b are quite close. There is also no clear consensus in the literature on the dependence of WAA on frequency. The residuals are displayed as box plots for different rain rate classes in Figure 6.

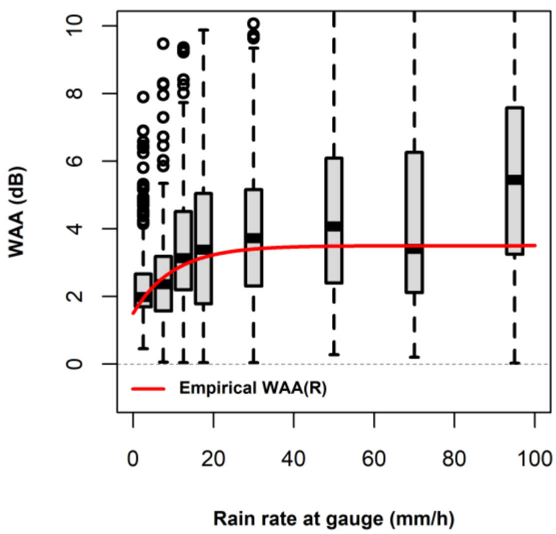

Figure 6 : Box plots of the residual between the attenuation measured by the link (A_{rain}) and the PIA expected from the measured rain rate (PIA_{Gauge}) as a function of the rain rate measured at the gauge. The original distribution contains 2712 points. The red line is the proposed empirical WAA(R) model, described in the text.

The overall shape of Figure 6 is compatible with an exponential model for WAA as a function of rain rate. A type of model which has been proposed by previous authors (Kharadly and Ross, 2001 ; Leijnse et al., 2008) with an offset plus a component increasing with rain rate and an asymptotical value at high rate :

https://doi.org/10.5194/egusphere-2026-2962
Preprint. Discussion started: 20 July 2026

$$WAA(R) = 2 \cdot \left[A_{max} - (A_{max} - A_0) \cdot e^{-\frac{R}{R_0}}\right] \quad (9)$$

The factor 2 is for the 2 antennas.

The 3 parameters were adjusted to the following values

- A_0 = 0.75 dB
- A_{max}= 1.5 dB
- R_0=10 mm/h

With these values the offset (initial WAA) is equal to 1.5 dB and the maximum WAA to 3 dB.

Several points are worth mentioning:

- first we acknowledge of the method used to set up the WAA model is empirical and rather subjective. We are faced with a limited data set, with one rain gauge per link at most and not situated directly below the link. The representativity of a single rain gauge measurement, in a region marked by highly variable rainfall is questionable. There is no direct (on site measurement) or indirect (ancillary data like radar or gauge at each end of the link) measurement of WAA. The used approach is pragmatic.
- Figure 6 shows a large spread in the distribution of the residual especially for high values of the rain rate. Fitting a function in such a spread data set is not satisfactory. However, as discussed in the next sections accounting for WAA even with an imperfect model does improve substantially the final rainfall estimation.
- We are aware that what we call a WAA model could be a way to compensate other source of errors such as the bias introduced by the coarse the quantization step (1dB), as discussed by other authors (Ostrometzky et al., 2017, Zinevich et al., 2010).

From Equations 7 and 9, estimating the rain rate from the CML attenuation is equivalent to solving the following equation :

$$A_{rain} = aR^b * L + A_{wa} = aR^b * L + 2 * (\ A0 + (Amax - A_0) * (1 - e^{-\frac{R}{R_0}})) \quad (10)$$

In practice the equation is solved by numerical solver (for instance the function uniroot from R).

3.5 CMLs processing chain summary

In summary the stages of the processing are :

- acquire the RSL mean data at the 15 minutes time resolution

- determine the baseline level as the mode of the raw attenuation over a 24 h time window.
- filter out misfunctioning links on the basis of maximum acceptable rain rate (250 mm/h) and low correlation with their neighbours.
- apply the WAA correction and estimate rain rate based on Equation 10.

The figures 7 and 8 illustrate the rain rate over the network for the first event, as in Figure 3 and 4, after outliers filtering and WAA correction. The improved agreement between the CMLs and the rain gauges is visible on the heat maps, in terms of rain occurrence (Figure 7) and rain rates (Figure 8). In Figure 7 the number of rainy time steps detected by the CMLs is very consistent with the gauges. The many false detections that appeared in Figure 3 up to several hours after the event have disappeared. The agreement in terms of rain rate values is also improved. The overall bias and the spread among the links is much reduced. The trend seen in Fig.4 of a positive bias increasing with shorter links has disappeared.

It is noteworthy that the 2 gauges themselves, though only 3 km apart, did not record the same event duration (4h30 for one, 5h30 for the other – cf Table 1) nor the same maximum rain rate (33 mm/h for one and 58 mm/h for the other), putting in perspective the difference between CMLs and gauges.

The results are similar for the nine other rain events (see supplement material, Figure S1).

Figures 7 and 8 provide a visual appreciation of the CMLs performances; the next section provides a statistical analysis of the results based on CML-gauge 15 minutes times series for the 10 recorded events.

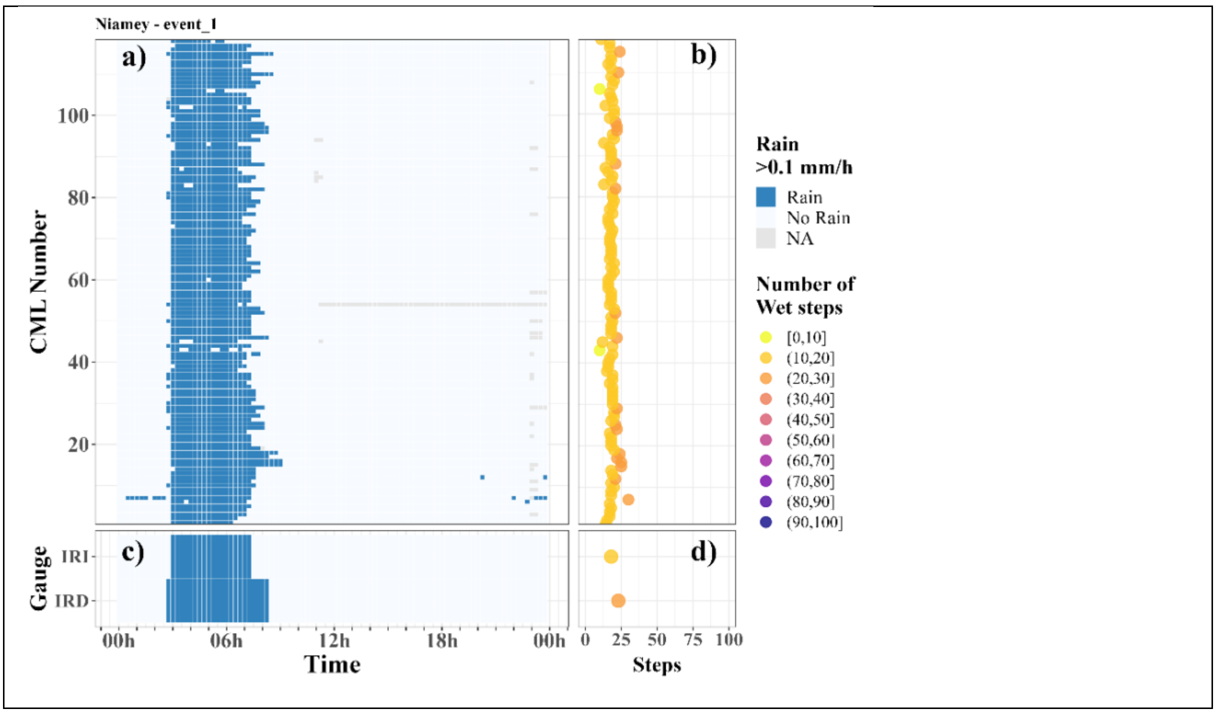

https://doi.org/10.5194/egusphere-2026-2962
Preprint. Discussion started: 20 July 2026

Figure 7: same as Figure 3 but after filtering of the outliers and application of the WAA correction.

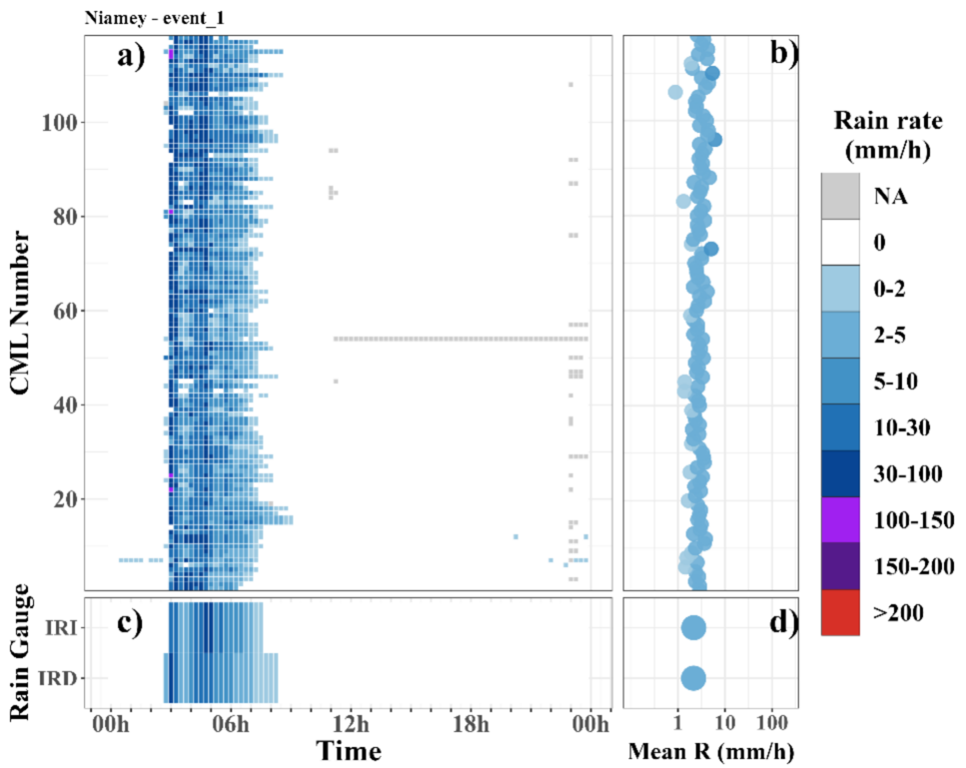

Figure 8: same as Figure 4 but after filtering of the outliers and application of the WAA correction.

https://doi.org/10.5194/egusphere-2026-2962
Preprint. Discussion started: 20 July 2026

4. CML base estimation assessment against gauges

The rainfall estimates derived at each link following the process described in section 2, have been compared with the rainfall recorded by the closest gauge. The comparisons are carried out for the 10 major events recorded by the gauges in 2017 and listed in Table 1. All comparisons and scores presented have been calculated with the 15 minutes time step.

4.1. Global statistics

Rain rate retrieval:

Global comparisons of the rain rates over the whole period, 43 hours of rain, are first derived. A scatter plot gathering all these link-gauge pairs over their common time steps is displayed in Figure 9a. This quantitative evaluation is carried out for all the links whose centre is located within 2 km from their closest rain gauge (29 links altogether). Only the time steps where at least one of the sensors (gauge or link) recorded non zero rainfall are shown, with a total of 4257 points. The other 5 plots in Figure 9 are for sub-categories of frequencies, 18-19 GHz for b-c and 22-23 GHz for d-e-f , and link lengths, as indicated in the titles. The overall performance for all links at 15-minute resolution is very good, the correlation coefficient is 0.87 and the normalized bias is 0. This compares well with the few other studies that reported results at small time steps (Chwala et al., 2012; Doumounia et al., 2014) and even with scores obtained at longer time steps (Overeem et al., 2011b; Pudashine et al., 2021). At the hourly time step the correlation is even higher (0.91, not shown).

Whatever the frequency and the link lengths, the correlations are very high. In terms of bias, the 25 links operating in the frequency range 22-23 GHz show slightly better performances than the 4 links operating at 18-19 GHz. The lower bias (-1%) is obtained for the links in the frequency range 22-23 GHz and length 1-2 km. The data sample is however not sufficient to draw general conclusions on the 'best' links. Better performance may be obtainable for shorter and longer links with a different set of algorithm parameters. Higher uncertainties for shorter links can be explained by an imperfect correction of the WAA (relatively more sensitive for short links). The uncertainty brought by the coarse quantization level (1 dB) is also relatively higher for the shortest links. Based on the *a, b* values in Table 2, we can derive from -Eq. 6 - that a PIA increment of 1 dB is equivalent to 15 mm/h for a 0.5 km long, 22 GHz link, and to 4 mm/h for a 2 km/22 Ghz link.

In Figure 9 some spread is visible for the highest rain rates (above 50 mm/h) ; it can be partly explained by the limitation in comparing a link with a single gauge during the highly variable convective rainfall peak. Table 1 shows some significant disagreement among the maximum rain rates recorded by the two central rain gauges which are only 3 km apart.

https://doi.org/10.5194/egusphere-2026-2962
Preprint. Discussion started: 20 July 2026

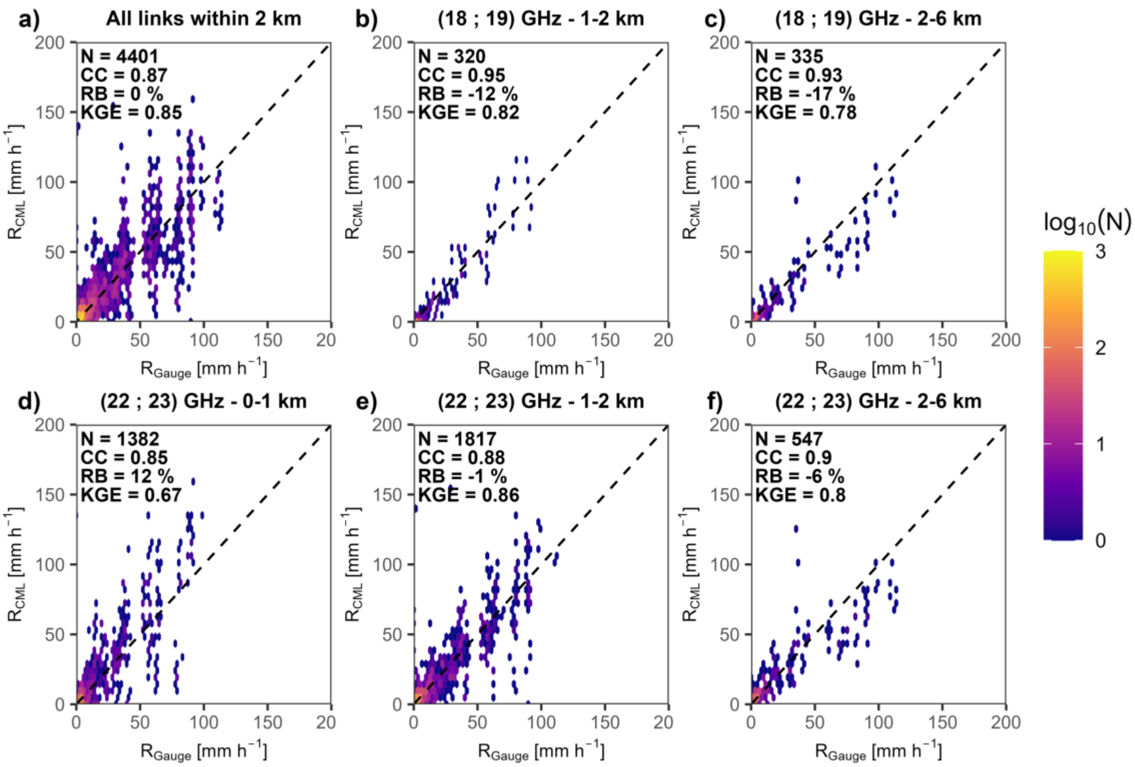

Figure 9 : Scatter plot of the rain rates retrieved by the CMLs (Y axis) and the closest gauge (X axis) at the 15 minute time step for all links within 2 km of a gauge (a) and for subset of frequencies and lengths (b-f), as indicated on the plots.

Categorical scores:

The ability of the CMLs to detect rainfall of different intensity is illustrated in Figure 10.

The Probability of Detection (POD) and False Alarm Ratio (FAR) are derived, for four different rain rate thresholds (0, 2, 5 and 10 mm/h).

– Probability of Detection (POD)

$$POD = \frac{H}{H + M}$$

– False Alarm Ratio (FAR)

$$\boldsymbol{FAR} = \frac{\boldsymbol{FP}}{\boldsymbol{H} + \boldsymbol{FP}}$$

With H, M and FP defined in Table 3.

Thr = 0,2, 5 or 10 mm/h	R_{Gauge} > Thr	$R_{Gauge} \leq$ Thr
R_{CML} > Thr	Hit (H)	False Positive (FP)
$R_{CML} \leq$ Thr	Miss (M)	Correct Negative (NEG)

Table 3 : categorical score variables definition.

The scores are displayed in Figure 10 for 3 classes of link length : a) less than 1 km, b) 1 to 2 km, c) 2-6 km.
For all links, the detection of the convective rainfall, above 5 mm/h is very good, with POD above 0.80. This is an important result given the importance of these intense rain rates that represent about 80 % of the rain accumulation in Sahel and are the causes of frequent flooding in Niamey. The FAR for these intense rainfall is however high, especially in the case of very small links. Lighter rain rates are partly missed, by 25-30% for links longer then 1 km and by about 35 % for shorter links. Given the coarse quantization step (1 dB) the detection of the lowest rain rate is a challenge (Turko et al., 2021), especially for the shortest links. The problem may be partly compensated by the WAA which can help the total attenuation by rain (Eq 7) to jump above the detectable value (1 dB). Conversely, the FAR for rain rates below 5 mm/h is very low.

These numbers are very satisfactory considering the spatial sampling difference between links and gauges.

https://doi.org/10.5194/egusphere-2026-2962
Preprint. Discussion started: 20 July 2026

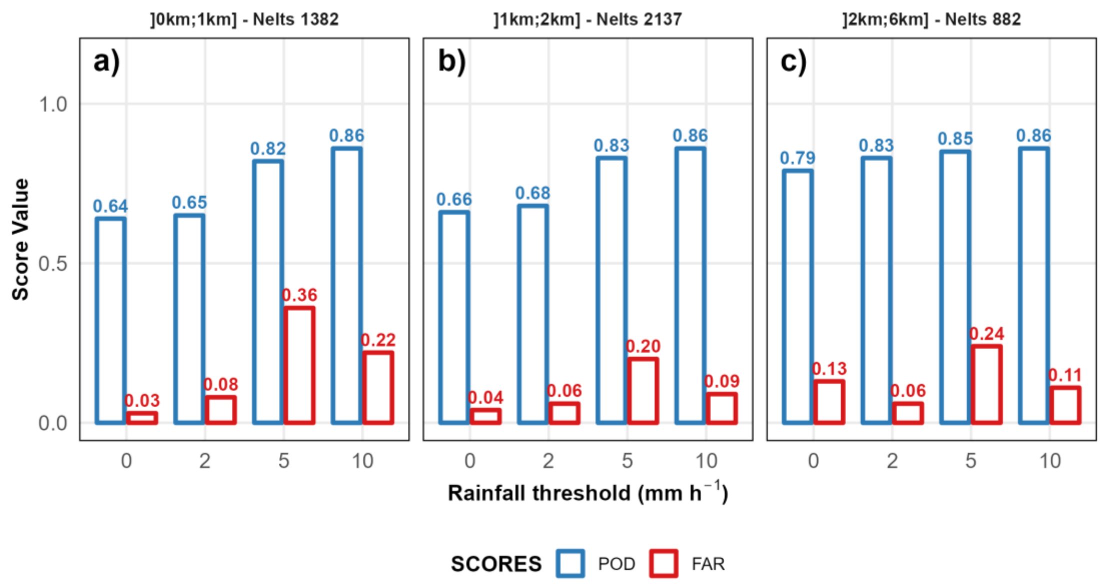

Figure 10 : POD and FAR for the indicated threshold of rain rate (0, 2, 5 or 10 mm/h) and three classes of link length (a) less than 1 km, b) 1 to 2 km, c) 2-6 km.

4.2. Frequency Distribution of rain rates

The capacity of the network to reproduce rainfall intensity statistics is important for many applications like the study of extreme events or flood risk assessment.

Figure 11 compares the frequency distributions of rain rates for all 144 links and the gauges. The agreement is better for the links longer than 1 km and for the convective rain rates (10 mm/h and above). The occurrence of rainfall rate below 5 mm/h is under-represented by the links. However, despite their high level of occurrence, rainfall below 10 mm/h represent a small contribution to the rain accumulation (Fig 11b and c) and for links longer than 1 km, there is a good agreement between the gauges and links for the rain rates in the range 10-100 mm/h that account for more than 80 % of the total rain.

https://doi.org/10.5194/egusphere-2026-2962
Preprint. Discussion started: 20 July 2026

a) L =< 1km

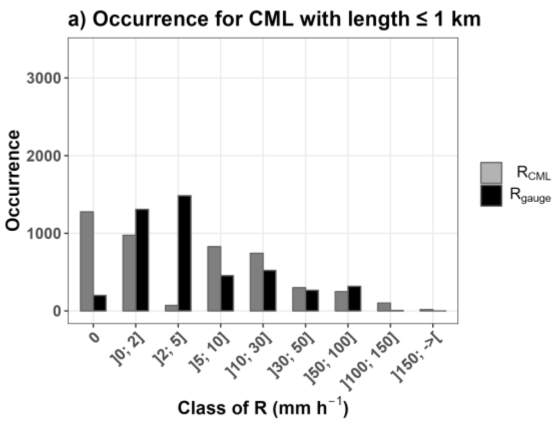

b) L > 1km

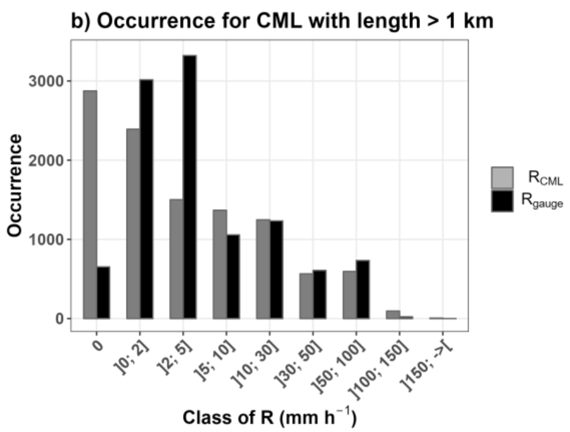

c) L =< 1km

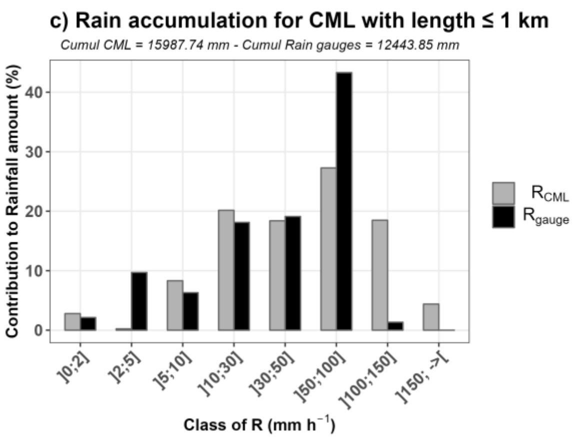

d) L > 1km

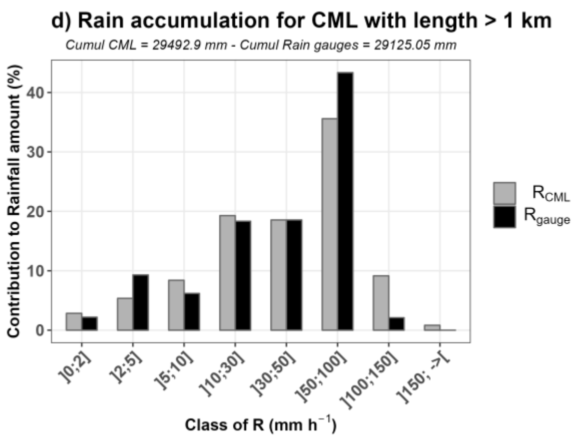

Figure 11 : frequency distribution of the rain rates retrieved by the links (grey) and the gauge (black) for the whole data set (10 events). a-b) frequency distribution and c-d) contribution to the total accumulation. Left) plots for Links shorter than or equal to 1 km, Right) Links longer than 1 km.

https://doi.org/10.5194/egusphere-2026-2962
Preprint. Discussion started: 20 July 2026

4.3. Overall behaviour of the network per event

The global statistics may hide some discrepancy among links, or rain events, that could be important in an operational context. Figure 12 shows the distribution of the correlations between individual links and their closest gauge, for each 10 events, when considering only links within 2 km of a gauge. For most events and most links, the correlation are above 0.85, and above 0.95 for the events 3,4 and 9. This is higher than the correlation of 0.84 observed between the 2 gauges, that are only 3 km apart (cf supplementary Figure S1).

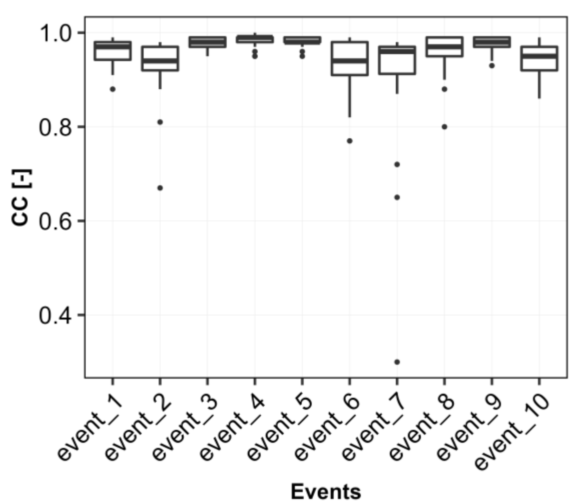

Figure 12: distribution of the correlation coefficients calculated between each link and the closest rain gauge, for each 10 events. Only the links with 2 km of a gauge are considered.

The correlations are lower when considering links which are further away from the gauges, as expected given the spatial structure of the convective rainfall in Sahel. However, robust information on the mean rainfall over Niamey can be derived from the ensemble of all links.

Figure 13 displays event hyetograph constructed by taking the interquartile range of rain rates over the entire network for 2 events (see supplementary Figure S11 for all events). For each time step, the quartile (25, 75 and median) of CML estimates are plotted against the average of the gauges, over Niamey area. The correlation of the daily series are indicated (when all links or only those distant from less than 2 km are considered), with values above 0.9 for the median of all links. For most events the rain gauge series is within the spread of the CMLs, and close to the median, suggesting that the median could be used as a

https://doi.org/10.5194/egusphere-2026-2962
Preprint. Discussion started: 20 July 2026

robust estimator of the average rainfall over the city and the interquartile as an indicator of the variability. This is an example of an urban scale rain product that can be derived easily, and well suited for operational applications.

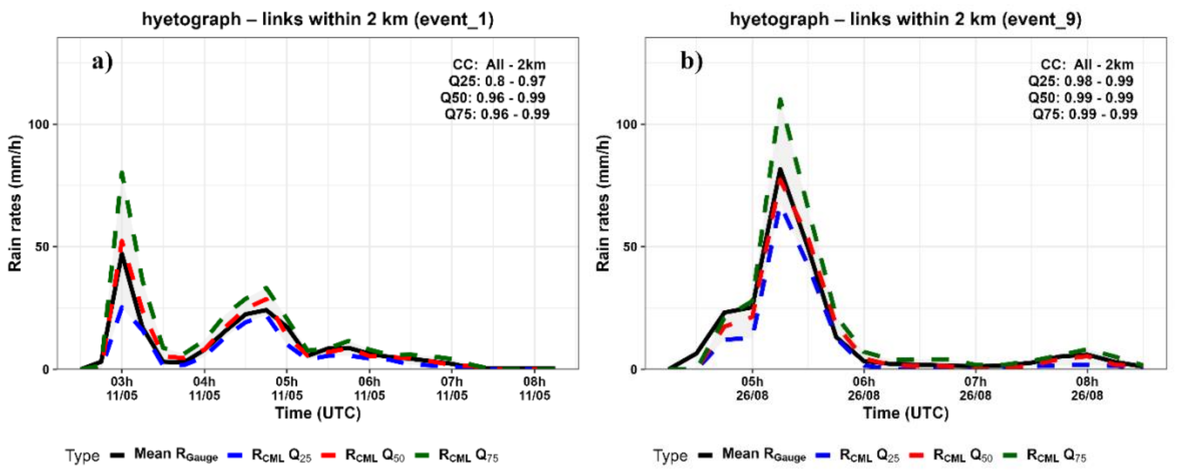

Figure 13: event hyetograph based on the quartile (median=red; 25th=blue; 75th=green) of link estimates, for links situated with 2 km of the gauges and gauge mean (black).
The correlation coefficient between the links quartiles and the gauge mean series are also indicated on each plot, considering all the links or only the links within 2 km.

Finally, Figure 14 illustrates the interest of the dense network of CMLs to monitor rainfall spatial variability. The example is for the event 8, where an extreme gradient of rainfall was observed within the city. Table 1 already shows the contrast between the 2 gauges, in terms of duration (11hours for one gauge and 7 hours for the other), intensity (78 or 90mm/h maximum rain rate) and accumulation (49 mm or 76 mm). The CMLs reveals that the MCS impacted only the south-east of the city, where the intense convective rainfall are seen around 12 pm (Fig. 14 c, d) with no rain in the northern part.

https://doi.org/10.5194/egusphere-2026-2962
Preprint. Discussion started: 20 July 2026

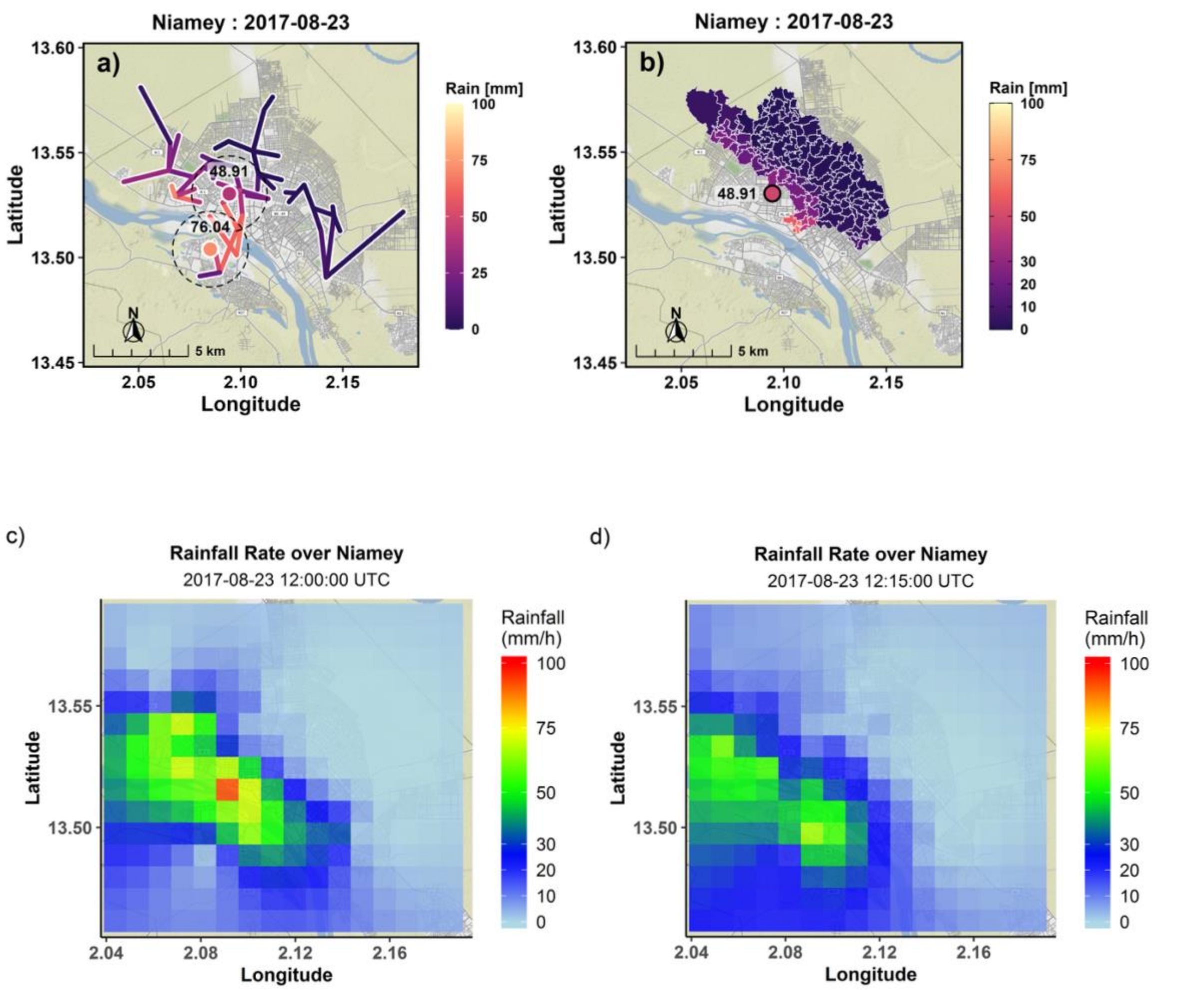

Figure 14 : Illustration of rainfall spatial variability over Niamey for the 8th event. a) Total rainfall measured by each link, b) total rainfall interpolated over the hydrological basin and elementary sub-basins, of an urban river that overflowed during the event, c) and d) rainfall maps (1 km resolution) showing the extension of the intense rainfall front, as the convective part of the MCS is crossing the south-eastern districts of Niamey.

530

https://doi.org/10.5194/egusphere-2026-2962
Preprint. Discussion started: 20 July 2026

5. Conclusion

This study confirms on an extended data set, with 144 links and several days of rain, the interest of commercial microwave links in data sparse regions like sub-Saharan Africa. Here CML based rainfall estimates could be assessed at their native time resolution, 15 minutes, which is unusual under such latitude. At this resolution, the correlation between the CML and rain gauges is close to 0.9, with slight variations depending on the frequencies and length considered. This high level of correlation is stable among the 10 events. When rainfall is estimated as the median value of the estimates from all links within 2 km of the gauges, the correlations are close to 0.99 for all events. The overall bias is close to 0. The bias varies if subcategories of links are considered. The lowest bias is obtained with links in the length range 1-2 kms and frequency 22-23 GHz. The capacity of detection is about 70 % for low rain rates (up to 2 mm/h) and reached 90% for the intense convective rainfall (from 10 m/h). The false alarm rate is below 10% (except in the category 2-5 mm/h). The frequency distribution of rain rates is well represented by the links in the convective range (above 10 mm/h) but the links tend to underestimate the occurrence of small to medium rain rates. However, the total amount of rain brought by each intensity class is well represented.

Ten rainfall events accounting for 80 % of the total rainfall in 2017 were analysed.

All the analysed events are associated with deep convection organized in Mesoscale convective systems (MCS), an important feature of tropical climate (Prein et al., 2024; Roca and Fiolleau, 2020). MCSs are characterized by intense precipitation and often responsible for flooding (Guehi et al., 2026). While the trajectories and cloud structure of these systems have been well observed by satellite (Fiolleau and Roca, 2024) quantifying and mapping the associated rainfall is still a challenge, by lack of operational radar network in the region. The scarcity of the operational rain gauge network limits the analysis of the spatial variability of these intense rainfall, especially at sub-daily scale, and this is a problem for characterizing extreme events (Guerreiro et al., 2018; Lengfeld et al., 2020). Here we have shown that a network of CMLs can provide precious high resolution information on the spatial and temporal characteristics of tropical rainfall. Such information could be useful for assessing the ability of satellite rainfall estimates and numerical weather models to represent tropical convection characteristics. They could also be used in many applications like urban hydrology (Turko et al., 2021).

Beyond the scientific outcomes which highlight on a new example the relevance and quantitative performances of the CML technique, under a variety of climates, the study provides new elements of perspective for the development of the CMLs technique in the global south and countries where technical expertise on rainfall measurement may not be available. An interesting point is that good performances were obtained with a very simple processing chain. The raw data were provided using the operator's own network monitoring system (NMS), requiring no external intervention on the network operation or computer system. The operator was able to configure the NMS to store data in real time (within 5 minutes of acquisition of the 15 minutes TSL/RSL) and push them on a ftp server. The old version of the equipment allowed acquisition of the TSL and RSL only with a coarse quantization step of 1 dBm. The method used for defining the baseline is very basic, based on the mode of the signal over a 24h window. One of the reasons for the good performance, despite limitations in the data and processing comes from the nature of the convective systems encountered in Niger. The rainy season is made of the succession of a few mesoscale convective systems separated by dry periods of several hours to days. Within these rainy events, most of the rainfall is provided by the intensive convective front, which creates an abrupt and easily detected attenuation peak in the CMLs signal. As the relative error in rainfall estimation which CMLs decreases with rain intensity – at least in the range of frequencies and length used in this study – this is also favourable for monitoring intense convective rain. While such favourable climatic conditions are not observed everywhere in Africa, they are common in the whole Sahelian region, which hosts some of the world populations most exposed to climatic risks and floodings. The perspective of investment in operational weather radar network and the human resources to operate them are very poor in this region, and solution based on the existing infrastructures like the telecommunication networks would be most relevant. The data presented in this study were obtained in a research framework, as part of a pilot demonstration. However, the proposed solution was implemented in real time and could easily be operationalized if an agreement was concluded with one (or several) telecommunication operators and a local institution. In order to facilitate the operational use of CMLs for rainfall estimation worldwide, a new initiative called the Global Microwave Data Initiative (GMDI; https://gmdi.eu/) is under discussion among several research institutes, telecommunication operators, national weather services and international authorities (WMO, ITU). Other collective initiatives to promote the CML technique towards a wider community of users include the development of publicly shared data and open source software packages (Chwala et al., 2026).

References

Alcoba, M., Gosset, M., Kacou, M., Cazenave, F., and Fontaine, E.: Characterization of Hydrometeors in Sahelian Convective Systems with an X-Band Radar and Comparison with In Situ Measurements. Part II: A Simple Brightband Method to Infer the Density of Icy Hydrometeors, Journal of Applied Meteorology and Climatology, 55, 251–263, https://doi.org/10.1175/JAMC-D-15-0014.1, 2016.

AMMA-CATCH : a hydrological, meteorological and ecological observatory on West Africa: AMMA-CATCH is labeled by the french institutes IRD and CNRS as “National Observation Service”. It is part of the french Research Infrastructure OZCAR., https://doi.org/10.17178/AMMA-CATCH.ALL, 1990.

https://doi.org/10.5194/egusphere-2026-2962
Preprint. Discussion started: 20 July 2026

Atlas, D. and Ulbrich, C. W.: Path- and Area-Integrated Rainfall Measurement by Microwave Attenuation in the 1–3 cm Band, J. Appl. Meteor., 16, 1322–1331, https://doi.org/10.1175/1520-0450(1977)016%253C1322:PAAIRM%253E2.0.CO;2, 1977.

Belloni, R., Camici, S., and Tarpanelli, A.: Towards the continuous monitoring of the extreme events through satellite radar altimetry observations, Journal of Hydrology, 603, 126870, https://doi.org/10.1016/j.jhydrol.2021.126870, 2021.

Berne, A. and Uijlenhoet, R.: Path-averaged rainfall estimation using microwave links: Uncertainty due to spatial rainfall variability, Geophysical Research Letters, 34, https://doi.org/10.1029/2007GL029409, 2007.

Casse, C., Gosset, M., Vischel, T., Quantin, G., and Tanimoun, B. A.: Model-based study of the role of rainfall and land use–land cover in the changes in the occurrence and intensity of Niger red floods in Niamey between 1953 and 2012, Hydrol. Earth Syst. Sci., 20, 2841–2859, https://doi.org/10.5194/hess-20-2841-2016, 2016.

Cazenave, F., Gosset, M., Kacou, M., Alcoba, M., Fontaine, E., Duroure, C., and Dolan, B.: Characterization of Hydrometeors in Sahelian Convective Systems with an X-Band Radar and Comparison with In Situ Measurements. Part I: Sensitivity of Polarimetric Radar Particle Identification Retrieval and Case Study Evaluation, Journal of Applied Meteorology and Climatology, 55, 231–249, https://doi.org/10.1175/JAMC-D-15-0013.1, 2016.

Chwala, C. and Kunstmann, H.: Commercial microwave link networks for rainfall observation: Assessment of the current status and future challenges, WIREs Water, 6, e1337, https://doi.org/10.1002/wat2.1337, 2019.

Chwala, C., Gmeiner, A., Qiu, W., Hipp, S., Nienaber, D., Siart, U., Eibert, T., Pohl, M., Seltmann, J., Fritz, J., and Kunstmann, H.: Precipitation observation using microwave backhaul links in the alpine and pre-alpine region of Southern Germany, Hydrology and Earth System Sciences, 16, 2647–2661, https://doi.org/10.5194/hess-16-2647-2012, 2012.

Chwala, C., Overeem, A., Øydvin, E., Petersson Wårdh, L., Seidel, J., Graf, M., Walraven, B., Covi, E., Habi, H. V., Fencl, M., de Vos, L., Giannetti, F., Green, A., O'Hara, T., Blettner, N., Keel, T., Schutz, G., El Hachem, A., Illich, N., Polz, J., Shit, T., Kaleta, L., Zulkarnaen, D., and Bareš, V.: Open-source tools for processing opportunistic rainfall sensor data: An overview of existing tools and the new OpenSense software packages poligrain, pypwsqc and mergeplg, EGUsphere, 1–31, https://doi.org/10.5194/egusphere-2025-5438, 2026.

David, N., Liu, Y., Kumah, K. K., Hoedjes, J. C. B., Su, B. Z., and Gao, H. O.: On the Power of Microwave Communication Data to Monitor Rain for Agricultural Needs in Africa, Water, 13, 730, https://doi.org/10.3390/w13050730, 2021.

Di Baldassarre, G., Montanari, A., Lins, H., Koutsoyiannis, D., Brandimarte, L., and Blöschl, G.: Flood fatalities in Africa: From diagnosis to mitigation, Geophys. Res. Lett., 37, L22402, https://doi.org/10.1029/2010GL045467, 2010.

Djibo, M., Chwala, C., Graf, M., Polz, J., Kunstmann, H., and Zougmoré, F.: High-resolution rainfall maps from commercial microwave links for a data-scarce region in West Africa, Journal of Hydrometeorology, 1, https://doi.org/10.1175/JHM-D-23-0015.1, 2023.

Doumounia, A., Gosset, M., Cazenave, F., Kacou, M., and Zougmore, F.: Rainfall monitoring based on microwave links from cellular telecommunication networks: First results from a West African test bed, Geophysical Research Letters, 41, https://doi.org/10.1002/2014GL060724, 2014.

Esmaeil Nia, S. and Shokri, A.: Exploring the impact of rainfall intensity on the attenuation-rainfall relationship, Journal of Quantitative Spectroscopy and Radiative Transfer, 334, 109364, https://doi.org/10.1016/j.jqsrt.2025.109364, 2025.

https://doi.org/10.5194/egusphere-2026-2962
Preprint. Discussion started: 20 July 2026

Fencl, M., Valtr, P., Kvicera, M., and Bares, V.: Quantifying Wet Antenna Attenuation in 38-GHz Commercial Microwave Links of Cellular Backhaul, IEEE Geosci. Remote Sensing Lett., 16, 514–518, https://doi.org/10.1109/LGRS.2018.2876696, 2019.

Fenicia, F., Pfister, L., Kavetski, D., Matgen, P., Iffly, J.-F., Hoffmann, L., and Uijlenhoet, R.: Microwave links for rainfall estimation in an urban environment: Insights from an experimental setup in Luxembourg-City, Journal of Hydrology, 464–465, 69–78, https://doi.org/10.1016/j.jhydrol.2012.06.047, 2012.

Fiolleau, T. and Roca, R.: A database of deep convective systems derived from the intercalibrated meteorological geostationary satellite fleet and the TOOCAN algorithm (2012–2020), Earth System Science Data, 16, 4021–4050, https://doi.org/10.5194/essd-16-4021-2024, 2024.

Galle, S., Grippa, M., Peugeot, C., Moussa, I. B., Cappelaere, B., Demarty, J., Mougin, E., Panthou, G., Adjomayi, P., Agbossou, E. k., Ba, A., Boucher, M., Cohard, J.-M., Descloitres, M., Descroix, L., Diawara, M., Dossou, M., Favreau, G., Gangneron, F., Gosset, M., Hector, B., Hiernaux, P., Issoufou, B.-A., Kergoat, L., Lawin, E., Lebel, T., Legchenko, A., Abdou, M. M., Malam-Issa, O., Mamadou, O., Nazoumou, Y., Pellarin, T., Quantin, G., Sambou, B., Seghieri, J., Séguis, L., Vandervaere, J.-P., Vischel, T., Vouillamoz, J.-M., Zannou, A., Afouda, S., Alhassane, A., Arjounin, M., Barral, H., Biron, R., Cazenave, F., Chaffard, V., Chazarin, J.-P., Guyard, H., Koné, A., Mainassara, I., Mamane, A., Oi, M., Ouani, T., Soumaguel, N., Wubda, M., Ago, E. e., Alle, I. c., Allies, A., Arpin-Pont, F., Awessou, B., Cassé, C., Charvet, G., Dardel, C., Depeyre, A., Diallo, F. b., Do, T., Fatras, C., Frappart, F., Gal, L., Gascon, T., Gibon, F., Guiro, I., Ingatan, A., Kempf, J., Kotchoni, D. o. v., Lawson, F. m. a., Leauthaud, C., Louvet, S., Mason, E., Nguyen, C. c., Perrimond, B., Pierre, C., Richard, A., Robert, E., Román-Cascón, C., Velluet, C., and Wilcox, C.: AMMA-CATCH, a Critical Zone Observatory in West Africa Monitoring a Region in Transition, Vadose Zone Journal, 17, 180062, https://doi.org/10.2136/vzj2018.03.0062, 2018.

Gosset, M., Kunstmann, H., Zougmore, F., Cazenave, F., Leijnse, H., Uijlenhoet, R., Chwala, C., Keis, F., Doumounia, A., Boubacar, B., Kacou, M., Alpert, P., Messer, H., Rieckermann, J., and Hoedjes, J.: Improving rainfall measurement in gauge poor regions thanks to mobile telecommunication networks, Bulletin of the American Meteorological Society, 97, https://doi.org/10.1175/BAMS-D-15-00164.1, 2016.

Guehi, F. J., Jucá Oliveira, R. A., Gosset, M., Kacou, M., Zahiri, E.-P., and Fiolleau, T.: A revisit of Niger river's major flood events and the role of convective systems with satellite data and hydrological modeling, Journal of Hydrology: Regional Studies, 63, 103025, https://doi.org/10.1016/j.ejrh.2025.103025, 2026.

Guerreiro, S. B., Fowler, H. J., Barbero, R., Westra, S., Lenderink, G., Blenkinsop, S., Lewis, E., and Li, X.-F.: Detection of continental-scale intensification of hourly rainfall extremes, Nature Clim Change, 8, 803–807, https://doi.org/10.1038/s41558-018-0245-3, 2018.

Guilloteau, C.: Approche physico-statistique de la désagrégation des précipitations satellite dans les Tropiques, phdthesis, Université Paul Sabatier - Toulouse III, Toulouse, France., 223 pp., 2016.

Harel, O., David, N., Alpert, P., and Messer, H.: The Potential of Microwave Communication Networks to Detect Dew—Experimental Study, IEEE J. Sel. Top. Appl. Earth Observations Remote Sensing, 8, 4396–4404, https://doi.org/10.1109/JSTARS.2015.2465909, 2015.

Heistermann, M., Jacobi, S., and Pfaff, T.: Technical Note: An open source library for processing weather radar data (wradlib), Hydrol. Earth Syst. Sci., 17, 863–871, https://doi.org/10.5194/hess-17-863-2013, 2013.

Henning, R. E. and Stanton, J. R.: Effects of dew on millimeter-wave propagation, in: Proceedings of SOUTHEASTCON '96, SOUTHEASTCON '96, 684–687, https://doi.org/10.1109/SECON.1996.510158, 1996.

https://doi.org/10.5194/egusphere-2026-2962
Preprint. Discussion started: 20 July 2026

Houze, R. A., Jr.: Convective and stratiform precipitation in the tropics, in: Tropical Rainfall Measurements (J. S. Theon and N. Fugono, Eds.), 27–35, 1988.

Imhoff, R. O., Overeem, A., Brauer, C. C., Leijnse, H., Weerts, A. H., and Uijlenhoet, R.: Rainfall Nowcasting Using Commercial Microwave Links, Geophysical Research Letters, 47, e2020GL089365, https://doi.org/10.1029/2020GL089365, 2020.

Israelsson, J., Black, E., Neves, C., Torgbor, F. F., Greatrex, H., Tanu, M., and Lamptey, P. N. L.: The spatial correlation structure of rainfall at the local scale over southern Ghana, Journal of Hydrology: Regional Studies, 31, 100720, https://doi.org/10.1016/j.ejrh.2020.100720, 2020.

ITU-R: RECOMMENDATION ITU-R P.838-3 Specific attenuation model for rain for use in prediction methods, International Telecommunication Union, ITU, Geneva, Switzerland, 2005.

Kharadly, M. M. Z. and Ross, R.: Effect of wet antenna attenuation on propagation data statistics, IEEE Transactions on Antennas and Propagation, 49, 1183–1191, https://doi.org/10.1109/8.943313, 2001.

Kidd, C., Becker, A., Huffman, G. J., Muller, C. L., Joe, P., Skofronick-Jackson, G., and Kirschbaum, D. B.: So, How Much of the Earth's Surface Is Covered by Rain Gauges?, Bulletin of the American Meteorological Society, 98, 69–78, https://doi.org/10.1175/BAMS-D-14-00283.1, 2017.

Kumah, K. K., Hoedjes, J. C. B., David, N., Maathuis, B. H. P., Gao, H. O., and Su, B. Z.: The MSG Technique: Improving Commercial Microwave Link Rainfall Intensity by Using Rain Area Detection from Meteosat Second Generation, Remote Sensing, 13, 3274, https://doi.org/10.3390/rs13163274, 2021.

Leijnse, H., Uijlenhoet, R., and Stricker, J. N. M.: Hydrometeorological application of a microwave link: 1. Evaporation, Water Resources Research, 43, https://doi.org/10.1029/2006WR004988, 2007.

Leijnse, H., Uijlenhoet, R., and Stricker, J. N. M.: Microwave link rainfall estimation: Effects of link length and frequency, temporal sampling, power resolution, and wet antenna attenuation, Advances in Water Resources, 31, 1481–1493, https://doi.org/10.1016/j.advwatres.2008.03.004, 2008.

Lengfeld, K., Kirstetter, P.-E., Fowler, H. J., Yu, J., Becker, A., Flamig, Z., and Gourley, J.: Use of radar data for characterizing extreme precipitation at fine scales and short durations, Environ. Res. Lett., 15, 085003, https://doi.org/10.1088/1748-9326/ab98b4, 2020.

Mahamadou, Y., Ouma, M., and Abidina, D.: Statistical Assessment of the Extreme Rainfall Event of 2024 in Maradi and Zinder of South-Eastern Niger, Int. J.Environ. Clim. Change., 16, 324–335, https://doi.org/10.9734/ijecc/2026/v16i45363, 2026.

Mathon, V., Laurent, H., and Lebel, T.: Mesoscale Convective System Rainfall in the Sahel, Journal of Applied Meteorology, 41, 1081–1092, https://doi.org/10.1175/1520-0450(2002)041<1081:MCSRIT>2.0.CO;2, 2002.

Messer, H., Zinevich, A., and Alpert, P.: Environmental monitoring by wireless communication networks, Science, 312, 713, https://doi.org/10.1126/science.1120034, 2006.

Mie, G.: Beiträge zur Optik trüber Medien, speziell kolloidaler Metallösungen, Annalen der Physik, 330, 377–445, https://doi.org/10.1002/andp.19083300302, 1908.

Moumouni, S., Gosset, M., and Houngninou, E.: Main features of rain drop size distributions observed in Benin, West Africa, with optical disdrometers, Geophysical Research Letters, 35, 1–5, https://doi.org/10.1029/2008GL035755, 2008.

Müller, M., Bližňák, V., and Kašpar, M.: Analysis of rainfall time structures on a scale of hours, Atmospheric Research, 211, 38–51, https://doi.org/10.1016/j.atmosres.2018.04.015, 2018.

Olsen, R., Rogers, D., and Hodge, D.: The aRbrelation in the calculation of rain attenuation, IEEE Transactions on Antennas and Propagation, 26, 318–329, https://doi.org/10.1109/TAP.1978.1141845, 1978.

Ostrometzky, J., Eshel, A., Alpert, P., and Messer, H.: Induced bias in attenuation measurements taken from commercial microwave links, in: 2017 IEEE International Conference on Acoustics, Speech and Signal Processing (ICASSP), 2017 IEEE International Conference on Acoustics, Speech and Signal Processing (ICASSP), New Orleans, LA, 3744–3748, https://doi.org/10.1109/ICASSP.2017.7952856, 2017.

Ostrometzky, J. and Messer, H.: Dynamic Determination of the Baseline Level in Microwave Links for Rain Monitoring From Minimum Attenuation Values, IEEE Journal of Selected Topics in Applied Earth Observations and Remote Sensing, 11, 24–33, https://doi.org/10.1109/JSTARS.2017.2752902, 2018.

Ostrometzky, J., Raich, R., Bao, L., Hansryd, J., and Messer, H.: The Wet-Antenna Effect—A Factor to be Considered in Future Communication Networks, IEEE Trans. Antennas Propagat., 66, 315–322, https://doi.org/10.1109/TAP.2017.2767620, 2018.

Overeem, A., Leijnse, H., and Uijlenhoet, R.: Measuring urban rainfall using microwave links from commercial cellular communication networks: MEASURING URBAN RAINFALL USING MICROWAVE LINKS, Water Resour. Res., 47, https://doi.org/10.1029/2010WR010350, 2011a.

Overeem, A., Leijnse, H., and Uijlenhoet, R.: Measuring urban rainfall using microwave links from commercial cellular communication networks: MEASURING URBAN RAINFALL USING MICROWAVE LINKS, Water Resources Research, 47, n/a-n/a, https://doi.org/10.1029/2010WR010350, 2011b.

Overeem, A., Leijnse, H., and Uijlenhoet, R.: Retrieval algorithm for rainfall mapping from microwave links in a cellular communication network, Atmospheric Measurement Techniques, 9, 2425–2444, https://doi.org/10.5194/amt-9-2425-2016, 2016.

Overeem, A., Leijnse, H., van Leth, T. C., Bogerd, L., Priebe, J., Tricarico, D., Droste, A., and Uijlenhoet, R.: Tropical rainfall monitoring with commercial microwave links in Sri Lanka, Environ. Res. Lett., 16, 074058, https://doi.org/10.1088/1748-9326/ac0fa6, 2021.

Panthou, G., Lebel, T., Vischel, T., Quantin, G., Sane, Y., Ba, A., Ndiaye, O., Diongue-Niang, A., and Diopkane, M.: Rainfall intensification in tropical semi-arid regions: the Sahelian case, Environ. Res. Lett., 13, 064013, https://doi.org/10.1088/1748-9326/aac334, 2018.

Prein, A. F., Feng, Z., Fiolleau, T., Moon, Z. L., Núñez Ocasio, K. M., Kukulies, J., Roca, R., Varble, A. C., Rehbein, A., Liu, C., Ikeda, K., Mu, Y., and Rasmussen, R. M.: Km-Scale Simulations of Mesoscale Convective Systems Over South America—A Feature Tracker Intercomparison, Journal of Geophysical Research: Atmospheres, 129, e2023JD040254, https://doi.org/10.1029/2023JD040254, 2024.

Pu, K. and Liu, X.: Precipitation measurements experiment using microwave links in Eastern China from October 2020 to March 2022, Journal of Hydrology, 643, 131922, https://doi.org/10.1016/j.jhydrol.2024.131922, 2024.

Pudashine, J., Guyot, A., Overeem, A., Pauwels, V. R. N., Seed, A., Uijlenhoet, R., Prakash, M., and Walker, J. P.: Rainfall retrieval using commercial microwave links: Effect of sampling strategy on retrieval accuracy, Journal of Hydrology, 603, 126909, https://doi.org/10.1016/j.jhydrol.2021.126909, 2021.

Rahimi, A. R., Holt, A. R., Upton, G. J. G., and Cummings, R. J.: Use of dual-frequency microwave links for measuring path-averaged rainfall, J. Geophys. Res., 108, 2002JD003202, https://doi.org/10.1029/2002JD003202, 2003.

Roca, R. and Fiolleau, T.: Extreme precipitation in the tropics is closely associated with long-lived convective systems, Commun Earth Environ, 1, 1–6, https://doi.org/10.1038/s43247-020-00015-4, 2020.

Roversi, G., Alberoni, P. P., Fornasiero, A., and Porcù, F.: Commercial Microwave Links as a tool for operational rainfall monitoring in Northern Italy, https://doi.org/10.5194/amt-2020-43, 2020.

Schleiss, M. and Berne, A.: Identification of Dry and Rainy Periods Using Telecommunication Microwave Links, IEEE Geoscience and Remote Sensing Letters, 7, 611–615, https://doi.org/10.1109/LGRS.2010.2043052, 2010a.

Schleiss, M. and Berne, A.: Identification of Dry and Rainy Periods Using Telecommunication Microwave Links, IEEE Geoscience and Remote Sensing Letters, 7, 611–615, https://doi.org/10.1109/LGRS.2010.2043052, 2010b.

Schleiss, M., Rieckermann, J., and Berne, A.: Quantification and Modeling of Wet-Antenna Attenuation for Commercial Microwave Links, IEEE Geoscience and Remote Sensing Letters, 10, 1195–1199, https://doi.org/10.1109/LGRS.2012.2236074, 2013.

Song, K., Liu, X., and Gao, T.: Real-Time Rainfall Estimation Using Microwave Links: A Case Study in East China during the Plum Rain Season in 2020, Sensors, 21, 858, https://doi.org/10.3390/s21030858, 2021.

Taylor, C. M., Belušić, D., Guichard, F., Parker, D. J., Vischel, T., Bock, O., Harris, P. P., Janicot, S., Klein, C., and Panthou, G.: Frequency of extreme Sahelian storms tripled since 1982 in satellite observations, Nature, 544, 475–478, https://doi.org/10.1038/nature22069, 2017.

Tellman, B., Sullivan, J. A., Kuhn, C., Kettner, A. J., Doyle, C. S., Brakenridge, G. R., Erickson, T. A., and Slayback, D. A.: Satellite imaging reveals increased proportion of population exposed to floods, Nature, 596, 80–86, https://doi.org/10.1038/s41586-021-03695-w, 2021.

Tramblay, Y., Villarini, G., and Zhang, W.: Observed changes in flood hazard in Africa, Environ. Res. Lett., 15, 1040b5, https://doi.org/10.1088/1748-9326/abb90b, 2020.

Tramblay, Y., Villarini, G., Saidi, M. E., Massari, C., and Stein, L.: Classification of flood-generating processes in Africa, Sci Rep, 12, 18920, https://doi.org/10.1038/s41598-022-23725-5, 2022.

Turko, M., Gosset, M., Kacou, M., Bouvier, C., Chahinian, N., Boone, A., and Alcoba, M.: Rainfall Measurement from Commercial Microwave Links for Urban Hydrology in Africa: A Simulation Framework for Sensitivity Analysis, Journal of Hydrometeorology, 22, 1819–1834, https://doi.org/10.1175/JHM-D-20-0163.1, 2021.

Uijlenhoet, R., Overeem, A., and Leijnse, H.: Opportunistic remote sensing of rainfall using microwave links from cellular communication networks, WIREs Water, 5, e1289, https://doi.org/10.1002/wat2.1289, 2018.

Upton, G. J. G., Holt, A. R., Cummings, R. J., Rahimi, A. R., and Goddard, J. W. F.: Microwave links: The future for urban rainfall measurement?, Atmospheric Research, 77, 300–312, https://doi.org/10.1016/j.atmosres.2004.10.009, 2005.

van Leth, T. C., Overeem, A., Leijnse, H., and Uijlenhoet, R.: A measurement campaign to assess sources of error in microwave link rainfall estimation, Atmos. Meas. Tech., 11, 4645–4669, https://doi.org/10.5194/amt-11-4645-2018, 2018.

Vischel, T., Quantin, G., Lebel, T., Viarre, J., Gosset, M., Cazenave, F., and Panthou, G.: Generation of High-Resolution Rain Fields in West Africa: Evaluation of Dynamic Interpolation Methods, Journal of Hydrometeorology, 12, 1465–1482, https://doi.org/10.1175/JHM-D-10-05015.1, 2011.

Walraven, B., Overeem, A., Coenders-Gerrits, M., Hut, R., Valk, L. van der, and Uijlenhoet, R.: Relating Rainfall Retrieval Parameters to Network and Environmental Features to Improve Rainfall Estimates from Commercial Microwave Links in the Tropics, Journal of Hydrometeorology, 25, 1769–1791, https://doi.org/10.1175/JHM-D-24-0023.1, 2024.

Wenzel, M., Vogel, C., Graf, M., Winterrath, T., and Chwala, C.: Development of a Python Framework (pyRadman) for QPE using radar and CML data at DWD, Copernicus Meetings, https://doi.org/10.5194/egusphere-egu23-13779, 2023.

Yapi, N. A., Gosset, M., Kacou, M., Zahiri, É.-P., Alcoba, M., Boubacar, H., Happy, P., and Assamoi, P.: Estimation des précipitations via les réseaux de téléphonie mobile : exemple en Afrique subsaharienne, Météorologie, 55–62, https://doi.org/10.37053/lameteorologie-2023-0043, 2023.

Zhang, P., Liu, X., and Pu, K.: Precipitation Monitoring Using Commercial Microwave Links: Current Status, Challenges and Prospectives, Remote Sensing, 15, 4821, https://doi.org/10.3390/rs15194821, 2023.

Zinevich, A., Messer, H., and Alpert, P.: Prediction of rainfall intensity measurement errors using commercial microwave communication links, Atmospheric Measurement Techniques, 3, 1385–1402, https://doi.org/10.5194/amt-3-1385-2010, 2010.

https://doi.org/10.5194/egusphere-2026-2962
Preprint. Discussion started: 20 July 2026

Code and data availability

The data and code used to derive the plots are in the following temporary link .

https://dataverse.ird.fr/privateurl.xhtml?token=75bdbb88-07d8-4461-82a4-81e6028e5a87

The DOI for the final repository (not opened yet) is : https://doi.org/10.23708/RZMBFP .

Supplement link`

Supplement material is provided in a file. If and when the paper is accepted a link will be provided.

Author contributions

MG and MK carried out the analysis and prepared the manuscript. IR helped for code development and analysis.

Competing interests

We declare no competing interest.

Acknowledgements

The authors would like to thank the various people at the former company Orange Niger for their help in acquiring the data, and especially Boubacar. This work was developed as part of the International Research Network RAINSMORE financed by Institut de Recherche pour le Développement. The rain gauges are provided by the AMMA-CATCH observatory.